SSC PC-018
60 PAGES

Office of Research Administration
The University of Chicago
970 E. 58th Street
Chicago, Illinois 60637
(312) 702-8669

September 28, 1989

Mr. Tom Dombeck
SSC Division
ER-90
Department of Energy
Washington, D.C. 20545

The enclosed application is being submitted on behalf of the University of Chicago. Information regarding the submission is listed below:

TITLE OF PROJECT: "A Subsystem Proposal / Trigger for a Fast Solenoidal SSC Detector"

PRINCIPAL INVESTIGATOR: Henry J. Frisch /Melvyn Shochet

DEPARTMENT: Enrico Fermi Institute

DIVISION: Physical Sciences Division

UNIVERSITY GRANTS SYSTEM ID: 04260

To assist with processing, please cite the University's GRANTS system ID number as well as your reference number when submitting any correspondence regarding this project.

Thank you for your consideration of this proposal. If you need any assistance or further information, please call me at (312) 702-8601.

Sincerely,

Veena Agarwal

Veena Agarwal
Grant and Contract Management

enclosures

cc: Henry J. Frisch
John C Cole
Physical Sciences Division Administrator

September 28, 1989

A Subsystem Proposal for the Trigger for a Fast Solenoidal SSC Detector

Claudio Campagnari, Sarah Eno, Henry Frisch,† Carla Grosso-Pilcher, Marshall Miller, Harold Sanders, Melvyn Shochet† and Joe Ting
Enrico Fermi Institute, University of Chicago

Bob Ball, Myron Campbell‡ and J. Chapman†
Department of Physics, University of Michigan

Bruce Denby† and Eliane S. Lessner
Fermi National Accelerator Laboratory

Abstract

We propose to develop over the next three years a detailed design for a trigger system for a large solenoid detector with scintillator-based calorimeters, fast tracking, and muon detection. We propose to design and construct prototypes of detector-specific integrated circuits for the trigger system. Design considerations will include placement of electronics, generation of local trigger information, global trigger decisions, efficiencies and background rejection, and costs.

† Principal Investigator
‡ Principal Investigator and Contact Person

I. Introduction

The development of efficient triggers with large rejection factors will present one of the greatest challenges to the designers of SSC detectors. The success in meeting this challenge will determine the extent and quality of physics that can be derived from the SSC. We propose to design a trigger that incorporates the anticipated detector elements of a fast solenoidal detector into a multi-leveled trigger strategy. A survey of existing trigger systems and of technology from industry will be used to augment CDF based expertise. (see appendix A) We will analyze which subsystems are important for triggering and what is the optimum segmentation and precision required of each. In addition we propose the development of detector-specific integrated circuits to provide the low level trigger element generation needed to construct the general physics trigger. The areas of work for detector-specific integrated circuits includes fast track segment finders, neural network filters, and fast energy summation circuits.

II. System Design

The trigger system is difficult not only because it has a hard job to do, but also logistically, in that it interacts with many different subsystems of the detector. This implies many different interfaces, many control paths, and possible system problems such as ground loops, electronic noise and interference. It also is a system which can only be debugged fully under running conditions, when access to the detector is impossible. It is also hostage to the detector subsystems, in that it cannot function better than the signals provided it. Finally it is crucial - one cannot toss it overboard or delay it until the next run if it does not perform.

For all of these reasons a careful system design, with attention to operational aspects (how to diagnose it, control it, evade problems on the detector, etc.) is necessary. Before designing the CDF trigger we made a survey of the trigger systems on existing detectors (at CERN, DESY, SLAC, and Fermilab). We also looked carefully at existing and developing technology to identify what was most promising (e.g. the question of how early to digitize was heavily influenced by the state of flash-ADC's and of fast op-amps; the Level-2 design was partly determined by the anticipated availability of certain bit-slice processors.) We need to do this again, with particular attention paid to technology which will be cost effective, such as technology driven by the new high-resolution TV, for example.

A. Assumptions - We make the following assumptions regarding the nature of the detector and trigger. These assumptions are not completely general - they imply some decisions and judgements, but we believe they are reasonable.

1. The detector for which we are designing a trigger has a large solenoidal magnet, with cylindrical tracking chamber(s) inside, 4π calorimeter coverage, both electromagnetic and hadronic, and full muon coverage.

2. The calorimeters are constructed with scintillator (or an equivalently fast medium) with response times comparable or shorter than the SSC bunch spacing time. In the course of our study, we will consider the needed modifications (e.g., the use of leading edge timing information) if the chosen calorimeter technology is not sufficiently fast.

3. The tracking chambers and muon chambers have response times less than the pipeline times of the front-end electronics and can be used in the first level trigger. Scintillation counters may be necessary to augment large muon drift tubes.

4. The trigger should function comfortably at a luminosity of 10^{33}. The output rate should not have a contribution from the trigger hardware of more than 50% beyond what physics and detector would yield for an ideal trigger.

5. The trigger should be easily controlled and diagnosed; it should be simple and reliable, and yet flexible and robust. These wonderful words tend to be mutually exclusive - the development of dedicated VLSI chips which have the requisite trigger functions built directly into them is a major step toward achieving these goals by simplifying interconnects, and making a much smaller, more compact system.

6. The trigger will associate stiff tracks with calorimeter clusters and muons.

7. The calorimeter trigger will employ the same technique as developed for CDF to minimize the effect of energy fluctuations in a system of many individual towers. Only those towers which have energy greater than a tower threshold will be included in the trigger sum.

8. The trigger is intimately related to both the DAQ system and the front end electronics and must be coordinated with these systems as all three develop.

B. Design Decisions - We would like to have a design report finished after the first year. The design report should answer the following questions, among others:

1. What will be the quantities on which the final trigger decision is based?
2. Which subsystems will supply information to the trigger? (*e.g.*, if there are shower profile systems in the calorimeter, will they be used in the trigger? Other examples are the use of preconverters and of timing information)
3. What level of segmentation of trigger signals is necessary? (both transverse, and in depth. The question applies to all systems not just calorimeters) The answers to questions 2 and 3 are equivalent to a channel list for the trigger.
4. What level of precision is needed for the trigger information from each system?
5. How is the information from the detector stored while the trigger decision is being made?
6. At what stage does one go from analog to digital? This question is intimately related to question 5 above - analog makes for much more compact summing of channels at the front end, digital is fundamentally easier if the technology exists.
7. At what stage does one go from dedicated hardware to processors?
8. What is the output rate into the DAQ, and hence to higher level triggers?
9. How much is located on the detector and how much is accessible during collisions?
10. What is the system architecture?
11. What kinds of pattern recognition are needed?
12. Schedule and cost estimates.

III. Detector Specific Circuits

Because of the high channel count anticipated in SSC detectors, it will be necessary to develop inexpensive fast circuitry for the specific detectors being developed by the other subgroups. The development of first level trigger signals is integrally related to the detector characteristics. Significant coordination will be required for this process to be effective in developing the needed circuits. Some things are already clear, however; transverse energy sums will be required for calorimeter triggers and fast track segment finding with transverse

momentum selection will be necessary for lepton triggers. For tracking devices such as straw tubes and muon drift tubes, information about the crossing number will be required for association of the tracking data with the correct calorimetric data. Several members of this proposal are also members of detector subsystem proposals as a means of linking the detector and trigger efforts. (B.D. - Silicon Vertex; B.B. - Muons, Tracking: J.W.C. - Tracking)

Our goal is the development of a set of prototype integrated circuits that implement various trigger functions. One of the first devices to be built as an ASIC (Application Specific Integrated Circuit) will be a device used to aid in tracking devices, a synchronizer. (see appendix B) This device is used with multiple layers of drift tubes to generate both a drift time and a crossing time. A circuit for the generation of the calorimeter energy sums, weighted and unweighted, as needed for transverse and total energy, will be devised. A stiff track finder similar to that used in CDF is planned. It is anticipated that a single circuit can be devised that handles both the straw tube tracking problem and the large tube tracking problem representative of muon detectors. While the circuits to accomplish most of these functions are not new, the integration of them into custom ICs is both new and necessary given the number of channels required by SSC detectors.

IV. Pattern Recognition

At the SSC, there is a need for very fast, robust pattern recognition at the trigger level. Since the response times of most existing and foreseeable detectors is greater than the 16 ns bunch crossing time, when a trigger occurs, some of the signals read out from the detectors will indeed have come from the event which caused the trigger, but others will be portions of signals from previous or subsequent events which fall into the readout time window. The only difference between the in-time signals and the out-of-time signals is that the in-time signals will form plausible coherent spatial patterns, such as smoothly curving tracks that point at calorimeter clusters of appropriate energy, and the out-of-time ones will not. Pattern recognition is thus a special problem for the trigger at the SSC in the sense that we are obliged to perform it even to determine *which* data should be considered. The problem is exacerbated by the high probability of multiple interactions per bunch crossing at the SSC (46 percent of crossings have more than one interaction). In these cases it is also necessary to determine which data are associated with the interaction that produced the trigger. Our approach to the these problems will be to consider ways to

reduce the unwanted out of time signals as much as possible by the choice of fast detectors and by first level processing of the signals so as to minimize the crossing uncertainty. When crossing uncertainty remains after the first trigger level, pattern matching electronics will be enormously important in the reduction of data flow through the various trigger levels.

Most triggering schemes for the SSC propose a multi-level system. In the first level, prompt cuts, such as total E_T, missing E_T, number of clusters, presence of leptons, etc., will be used to produce a reduction of perhaps a factor of a few thousand. This leaves the additional factor of 10^4, needed to get the rate to tape to an acceptable level, up to higher levels of triggering, which will have to use non-prompt cuts, including 'physics' cuts. This implies that the higher levels at the SSC will rely very heavily on pattern recognition, since identification of particular topologies is usually what one means by 'physics' cuts. Such a rejection factor has never been obtained to date in a High Energy Physics collider experiment (CDF achieves a *total* reduction of about $5 \cdot 10^4$).

Some pattern recognition problems can be made relatively easy by the careful choice of detector design. Muon detection with chambers located outside many interaction lengths of iron is one example. Electron identification using stiff track information along with electromagnetic calorimeter information is another example. A third example is a missing E_T signature made by summing the total E_T over a hermetic detector.

Heavy quark spectroscopy is one domain in which the requirements placed on pattern recognition are more severe. The SSC running at a luminosity of 10^{32} and with a reconstruction efficiency for b-quark events of 1 percent is roughly equivalent to a 100 percent efficient e^+e^- B factory running at a luminosity of 10^{36}. B events will be 'soft', with a mean p_T of 6 GeV/c, and will produce decay leptons of only 1 to 2 GeV/c. In order to separate B events from the background, it will be necessary to use tracking and secondary vertex finding, at the trigger level.

The goal of the work in pattern recognition is twofold. The first is to exploit the physics signatures which come easily from the detector in conventional high speed processors incorporated within the overall system design. The second is to try to bring into use more sophisticated pattern recognition techniques used in other fields. Two of us (Denby and Campbell) have received Generic R&D funds for one year to investigate the use of neural networks for triggering. The motivations for this line of research, *e.g.*, pattern recognition

on sub-microsecond timescales, are described in detail in Appendix C, which is an updated version of the generic neural net proposal. We request here funds to allow these investigations to continue beyond the first year, within a highly experienced collaboration which is concurrently addressing the global question of triggering at the SSC.

We summarize here the activities in the neural net proposal:

A. Calorimetry based B Trigger.

A three layer, feed-forward neural net will be constructed which will, in the CDF calorimeter, differentiate background jets from jets containing an electron from the semileptonic decay of a B particle. There have been a number of interesting developments since the writing of the generic proposal:

1. We have simulated the required network on a general purpose Fortran neural net simulator of our design, and have trained the net using ISAJET generated B-jets and background events from real CDF data. The results, though still preliminary, are encouraging: the network correctly identifies about 65% of the jets which came from B decay while rejecting 95% of the background jets, based on samples of a few hundred events. We are continuing to run these simulations on larger data sets, experimenting with the parameters of the net.

2. Neural network chips of sufficient scale for this trigger are now commercially available from Hitachi, Oxford Computer, and Intel. The Intel chip, called a 64 Neuron ETANN (Electronically Trainable Analog Neural Network), which is optimized for processing speed, seems the most promising for our application. The chip can accept 128 analog inputs, and produces a trigger response about 4 microseconds after presentation of calorimeter data. We are currently involved in obtaining samples of these chips under a nondisclosure agreement and setting up test beds for them. This device should allow us to realize the calorimetry based B trigger more quickly and less expensively than supposed in our generic neural net proposal, since the chips themselves are not expensive, and all that remains are the analog shifters/receivers to get the signals out of the existing CDF trigger electronics.

3. We plan to instrument only the central region of the calorimeter to allow us to get a small scale prototype of the trigger up and working as soon as possible as a proof of technique.

B. Tracking and Particle identification.

1. Tracking. (see appendix C).

2. Secondary Vertex finding.

   We have made significant progress since the writing of the generic proposal. We used $B\bar{B}$ events generated by ISAJET assuming a 4 plane silicon vertex detector embedded in the CDF detector. We plot all tracks above .5 GeV p_T as points in the ϕ (azimuthal angle) versus D (impact parameter) plane. An example is shown in figure 1. In this transform plane, all tracks from the primary vertex fall on a horizontal line, while tracks from secondary vertices fall on lines which cross D=0 at some angle. A recurrent neural network was simulated which attempts to find the angled lines due to secondary vertices, after deletion of all tracks consistent with coming from the primary vertex. In the example of figure 1, the algorithm has found vertices coming from both B's present in the event.

   A preliminary study of this method as a B trigger yields the following results:

Bottom jets:		
30 Gev < p_T < 100 GeV	efficiency for B's:	70%
	background accepted:	0.26%
50 GeV < p_T < 100 GeV	efficiency for B's	81%
Top jets ($M_{top} = 100GeV$):		
30 GeV < p_T < 100 GeV	efficiency for B's	50%

   These studies are based upon samples of 200 Bottom events, 200 Top events, and 1500 background events. We are continuing these studies to see the effects of changing p_T cuts, acceptance cuts, worsened resolution, etc., but the initial results look quite promising. Although the Intel chip does not seem appropriate for this problem (due to the need to change the weights frequently), it should be possible to build neural net chips which, in conjunction with the associative memories being developed at Pisa, can find secondary vertices in a few microseconds. We will investigate the fabrication of such chips when the plans for the architecture have stabilized.

3. Stereo matching (see appendix C).

4. Čerenkov photon assignment (see appendix C).

5. Track segment finding in Straw chambers.

   This project should profit from a symbiotic relationship with the other straw tube projects outlined in this proposal. (see appendix C).

6. Hardware and algorithm research (see appendix C).

More generally, the neural network projects should benefit immensely from the close proximity to the projects outlined in this proposal which attack the triggering problem globally, and from the existence within this collaboration of integrated circuit fabrication facilities.

V. Custom IC Fabrication

The front end sampling, summing, comparison with threshold, and track segment finding should be done on a chip, rather than on a board as at present. We have at Michigan and Chicago extensive resources for chip development and testing. The MOSIS process of ASIC production will be undertaken with the goal that the needed chips be developed. We describe below the initial situation at Chicago and Michigan.

Recently at Chicago we have acquired three Apollo workstations with Mentor software for CAD design in order to upgrade the Telesis system we used for the CDF design. The workstations support the MOSIS package, which will allow us to design chips for the front end of the trigger. The workstations at Chicago have been in use for about a year producing printed circuit board designs. At Michigan we have two Apollo workstations running the same Mentor Graphics CAD software. The Mentor system is used by the Michigan Engineering School which has some 200 stations. Michigan has a complete IC fabrication laboratory that is available to us as well. The Physics Department at Michigan plans to purchase a third Mentor station with University funds in 1991. The Mentor software has been in use for printed circuit board and surface mount hybrid design for about a year in the Michigan Physics Department. An integrated circuit design has been developed but no circuit has yet been fabricated from such a design. We are familiar with the learning curve for new technology and expect that the first custom design will take considerable time to perfect. Test equipment for chips will be required since neither institution has such equipment presently.

We will want to prototype each kind of circuit in the system, providing test fixtures and external signals as closely matching those of the actual system as possible. This sequence of design, testing, and evaluation will require a major investment in test equipment. We will require the latest electronics technology, which moves very fast. We consequently want to work more on developing techniques and prototypes rather than on large quantities of actual production boards. As the details of trigger design take shape, we will utilize one of the existing temporal simulation languages to describe the trigger. The framework developed should prove indispensable for understanding the flow of data and trigger decisions as detector designs mature.

VI. Budget

A. University of Chicago

There is a large contribution to this project from the existing facilities and grants. The situation is one of high leverage, in that at Chicago we have a first-rate electronic shop, with two talented and experienced analog engineers who have built many trigger systems. We have recently invested in the Apollo workstations and Mentor software, and also have built up the infrastructure to deal with sophisticated CAD design and construction. Most importantly, there is a substantial group of physicists who have been working over the past many years (12 years , for two of us) developing a trigger which has performed well at a hadron collider at a luminosity of 2×10^{30}. This same group is now working on the upgrades which will allow triggering at luminosities of up to 10^{32}. Triggering at 10^{33}, with a 16 nsec bunch spacing, is a problem we have considered now for a long time (Shochet, Proceedings of the 1983 DPF Workshop on Collider Detectors, Berkeley 1983), and which we think we understand conceptually. To build up a group of this size from scratch to work on the trigger would cost many times what we are asking for in this proposal to supplement the existing facilities.

There are three main components in the budget: people, constructed equipment, and permanent equipment. We understand that our present support should carry the bulk of the personnel costs. We cannot add the load of designing an SSC trigger system by only redirecting people, however, as the hardware work they are doing is to upgrade the CDF trigger to handle higher luminosities (to within a factor of 10 of the SSC) and shorter bunch spacing. This work is directly on the path of the SSC trigger. Present personnel will spend

a substantial fraction of their time on the SSC, but we are already strapped to get the CDF work done on schedule. What is needed are two long-term professionals who can provide continuity over a long time span. We can rotate post-docs and students through the project picking off well-defined jobs, but we cannot ask junior people to work full-time on such a long-term project. We have consequently asked for a project engineer for the electronic shop to manage the technical aspects of the design under Harold Sanders' supervision, and an SRA who is full-time on the SSC to work closely with the other physicists who will have other responsibilities. (We estimate that the other physicists will spend between 15-20% of their time on the SSC on the average, with much of it being concentrated in intense periods of working largely on SSC projects.) We do not have the resources from our current support to add the long-term people we need to get the SSC job done.

The permanent equipment consists of test equipment for the ASIC chips we will design and build. We have the CAD tools, including the MOSIS software, already. The test equipment is spread over two years, with the basic logic analyzer in the first year, and the ASIC add-on option bought in the second year. The third year is a guess, based on the typical costs in the first two years.

The constructed equipment monies cover the costs of designing and constructing complete prototype boards. Labor for the design and construction, which is charged by the hour by our shop, is also included. The labor corresponds to approximately 1 FTE of technical support.

B. University of Michigan

Facilities and manpower for electronic circuit design and fabrication have been in place at Michigan for many years. About one year ago a newly renovated electronics shop area was made available to the High Energy Physics community. This space will continue to expand as additional nearby space becomes available as a result of the two fold increase in building space for Physics. The shop has the services of two electronics engineers and a supplies and fabrication supervisor.

The Michigan shop has provided designs, fabrication, and testing for a long list of circuits used in major experiments. A partial list of items follows:

1. 5000 channels of preamplifier - discriminator - TDCs for the HRS.
2. 3000 channels of high gain, low noise preamplifier - pulse shaper hybrids for the HRS.

3. Global trigger design for the HRS.
4. 1000 channels of hybrid preamplifiers for the MarkII small angle luminosity monitor, SAM.
5. Complete design of the MACRO event reconstruction processor, ERP.
6. Total design of the UMC muon system including high voltage distribution - preamplifier - and trigger system.

A foundation of experience and expertise is available at Michigan for this project within the constraints of the other activities being carried out in the same facility. The MACRO electronics work was recently awarded to the Michigan group as a result of an internal competition within the collaboration. A major part of the CDF muon upgrade electronics will be designed and fabricated in the shop as well. The D0 and L3 groups at Michigan also have projects scheduled for the shop as do the GRANITE and UMC experiments. The SSC trigger design effort cannot, therefore, be accomplished without some additional manpower. We have available through a large and prominent engineering school talented EECS graduate students and recent graduates. However, we feel that guidance for the project should be provided by a senior project engineer who will rely on the existing engineering, management, and fabrication support while directing the part time young talent that is available. We are requesting that such a senior director be supported by the project funds.

The maintenance of up to date electronics test equipment is challenging in a field that presses technology as steadily as does High Energy Physics. Our test equipment suffers this aging problem in a way that is compounded by the fact that much of the equipment was developed or purchased for and provided to facilities such as HRS, MarkII, UMC, and MACRO. Since these detectors are distant from our shop, the test equipment has been located at the detector site rather than in Ann Arbor. We are therefore very lean of test equipment generally and without fast modern IC test equipment entirely. We have, as a result, included in the budget several important IC specific items needed to augment the equipment that we have ordered under our regular DoE contract and from money provided by the University.

The existing generic grants will enable us to make progress towards some of the goals listed in this proposal. Substantial work has been done on the drift tube synchronizers and

work on the neural nets is just starting. Continuing these efforts with the help of a well equipped electronics shop and within the environment of a larger group concerned with trigger issues is clearly the next step in designing a trigger for the SSC.

C. Fermilab

In fields outside High Energy Physics, e.g., image analysis, hardware neural networks have shown the ability to perform pattern recognition tasks on the time scale of one microsecond. It is therefore logical to try to adapt this technology to pattern recognition in High Energy Physics, but the utility of neural networks in triggering is still to be demonstrated, as no one, to our knowledge, has yet used a neural network in an experimental trigger. If there exists anywhere a body qualified to assess this utility, it is the collaboration of the present proposal, as it combines the major neural net study group in High Energy Physics, based at Fermilab, with some of the most experienced trigger experts in the field. It is continuing support for this neural net study group that is sought here. (The Fermilab commitment is of course an institutional one, and additional Fermilab personnel may seek to join at a later date to work on any mutually agreeable part of the proposal.)

The group consists of Bruce Denby and one post-doc (in collaboration with M. Campbell and other personnel at Michigan), aided by programming support from E. Lessner and programming and hardware support from the Fermilab ACP group. In the first year much of the work will involve simulations of neural net triggers, and funds for an additional workstation are requested. We will also continue to acquire and gain familiarity with the commercial neural net circuits that are becoming available, and we request funds for the purchase of these chips and associated electronics. The primary focus will be upon the calorimetry based B trigger, implemented using the Intel ETANN circuit described earlier, in an effort to get a prototype up and working as soon as possible. The funds needed in following years will of course depend upon what is learned in the first year or two. If initial trials are successful, and if industrial progress continues in neural networks as quickly as it does today, neural networks may become a major component of SSC triggers, and correspondingly larger funds will be required.

MICHIGAN TRIGGER SUBSYSTEM BUDGET

	Year 1	Year 2	Year 3
1. SALARIES AND WAGES.....	$81,920	$88,170	$94,560
a. Project Engineeer (100% 12 months)	$35,000	$38,000	$41,000
b. Graduate Student Assistant (Physics) (50% 12 months)	$12,510	$13,200	$13,900
c. Graduate Student Assistant (EECS) (50% 12 months)	$12,510	$13,200	$13,900
Staff Benefits @ 20%	$12,000	$12,880	$13,760
Graduate Student Tuition Waivers	$9,900	$10,890	$12,000
2. PERMANENT EQUIPMENT.....	$43,230	$36,880	----
a. Digital Oscilloscope	$12,000	----	----
b. Logic Analyzer	$31,230	----	----
c. ASIC Prototype Verification Module	----	$36,880	----
3. TRAVEL (Domestic).....	$8,000	$8,000	$8,000
4. OTHER DIRECT COSTS.....	$79,500	$67,500	$87,500
a. MOSIS Chip Production ($10K per unit)	$10,000	$20,000	$30,000
b. Computer Simulation Costs	$20,000	$20,000	$20,000
c. Test Fixtures for ASICs	$10,000	$10,000	$10,000
d. Commercial Neural Network Chips	$6,000	$4,000	$4,000
e. Neural Network Test Fixtures	$30,000	$10,000	$20,000
f. Miscellaneous Expendable Materials & Supplies	$3,500	$3,500	$3,500
TOTAL DIRECT COSTS.....	$212,650	$200,550	$190,060
5. INDIRECT COSTS @ 33% modified Total Direct Costs.....	$55,909	$54,011	$62,720
TOTAL AMOUNT REQUESTED.....	$268,559	$254,561	$252,780

University of Chicago Trigger Subsystem Budget

	Year 1	Year 2	Year 3
Salaries and Wages	97,575	105,381	113,187
Henry Frisch	0	0	0
Melvyn Shochet	0	0	0
Senior Research Associate	35,000	38,000	41,000
Project Engineer	40,000	43,000	46,000
Fringe Benefits	22,575	24,381	26,187
Permanent Equipment	31,230	36,880	30,000
Logic Analyzer	31,230		
ASIC Prototype Verification Module		36,880	
Test Equipment			30,000
Travel	5,000	5,000	5,000
Other Direct Costs	75,000	93,000	106,000
Engineering and Electronics	50,000	53,000	56,000
MOSIS Chip Production ($10k/unit)	10,000	20,000	30,000
Test Fixtures for ASICs	10,000	10,000	10,000
Misc Expendable	5,000	10,000	10,000
EFI administrative Service	6,260	7,200	7,625
Indirect costs @65% modified TDC	73,993	82,928	88,278
Total	289,058	330,389	350,090

Fermilab Trigger Subsystem Budget

	Year 1	Year 2	Year 3
Salaries and Wages68,102	68,102	71,506	75,082
Post Doc	30,975	32,524	34,150
Bruce Denby (6 months)	22,733	23,869	25,063
Fringe Benefits	14,394	15,113	15,869
Permanent Equipment	10,000	0	0
Workstation	10,000		
Travel	5,000	5,000	5,000
Other Direct Costs	34,000	14,000	24,000
Commercial Neural Network Chips	4,000	4,000	4,000
Neural Network Test Fixtures	30,000	10,000	20,000
Total Direct Costs	117,102	90,506	104,082
Indirect costs @39% modified TDC	45,670	35,297	40,592
Total	162,772	125,803	144,674

Figure 1 - Finding two B vertices with a Neural Network

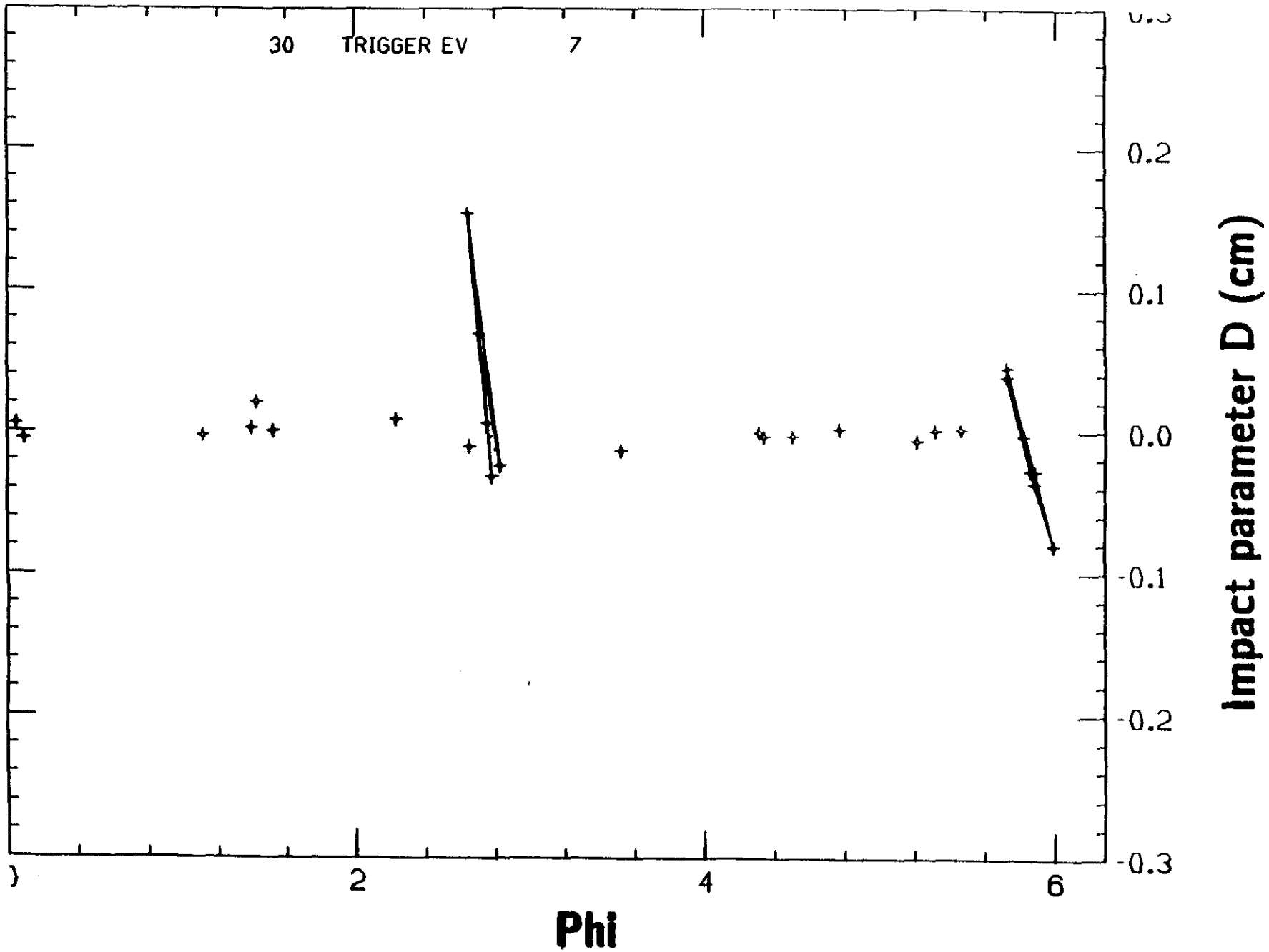

APPENDIX A

THE CDF TRIGGER

Nuclear Instruments and Methods in Physics Research A265 (1988) 326–335
North-Holland, Amsterdam

THE CDF TRIGGER

D. AMIDEI, M. CAMPBELL, H. FRISCH, C. GROSSO-PILCHER, J. HAUSER, T. LISS, G. REDLINGER, A. ROODMAN, H. SANDERS, M. SHOCHET, J. TING and Y.D. TSAI

The Enrico Fermi Institute and the Department of Physics, The University of Chicago, 5640 South Ellis Avenue, Chicago, IL 60637, USA

The trigger for the Collider Detector at Fermilab (CDF) is described. The detector is designed to study 2 TeV $p\bar{p}$ collisions at a luminosity of 10^{30} cm^{-2} s^{-1}. The interaction rate of 50 kHz is reduced by the trigger to the full event readout rate of 1–100 Hz.

1. Introduction

The CDF detector was designed to study the physics of $p\bar{p}$ interactions at a center of mass energy of 2 TeV. The detector has calorimeter coverage from 2° to 178° in polar angle and complete azimuthal coverage. The calorimeter consists of both electromagnetic and hadronic detectors [1]. The central part of the detector has a solenoid which generates a 15 kG axial magnetic field. A vertex time projection chamber and the 1.3 m radius central tracking chamber (CTC) are inside this field. A forward tracking chamber covers the polar angle region 2° to 10° [2].

The design luminosity for the Tevatron is 10^{30} cm^{-2} s^{-1}. An inelastic hadronic cross section of about 50 mb is expected at this energy. This may be compared with $\sim 13 \times 10^{-8}$ mb * at PEP. The expected interaction rate in CDF is then 50 kHz. It is expected that the rate of writing data to tape cannot exceed 1 Hz. Therefore, depending on the efficiency of online cuts, the trigger must reduce the rate by a factor of 5000 to 50000. This high reduction factor must take place through careful event selection since the expected rate of such interesting processes as W production and decay occur at only 0.002 Hz.

There were several criteria used in designing the trigger. The first is that it must accomplish the reduction in rate without rejecting any interesting known physics processes such as $Z^0 \to \mu^+\mu^-$ or $W \to e\nu$. The trigger must be capable of selecting processes that become interesting; it must be flexible in its selection criteria. Finally the trigger must be well matched to the strengths of the CDF detector, which are a finely segmented projective electromagnetic and hadronic calorimeter, excellent tracking and a strong magnetic field. The segmentation of the calorimeter is preserved in the trigger. Information from high P_T tracks in the CTC and muon system is also used in the trigger.

* This is the point-like cross section for μ-pairs. The hadronic cross-section is approximately four times as large.

0168-9002/88/$03.50 © Elsevier Science Publishers B.V. (North-Holland Physics Publishing Division)

2. Overview of operation

The segmentation of the CDF calorimetry is a function of the detector type and polar angle. The segmentation of the calorimetry for the trigger is a uniform 24×42 array, with a segmentation of 15° in ϕ and 0.2 units in rapidity. To match the different segmentations two central calorimeter cells, $15° \times 0.1$, are added together and 6 gas calorimetry cells, $5° \times 0.1$, are added to form one trigger tower. The signal for each trigger tower is scaled to 1 volt = 100 GeV. There are two arrays input to the trigger, one for electromagnetic energy and one for hadronic energy.

The muon and tracking systems are also mapped onto the 24×42 array. The central muon coverage extends from about 0.6 to −0.6 in rapidity. The forward muon system covers from about 1.8 to 4.0 and −1.8 to −4.0. The muon system is matched to the calorimetry by the trigger system to help identify isolated muon. A prompt hit track processor operating on the central detector also is used in the trigger. High P_T tracks are matched to the calorimetry in order to identify electrons. Information from the track processor is also matched to the central muon system in order to reject muon signals resulting from hadronic punch through. The outer layer of the CTC extends from −1.0 to +1.0 in rapidity.

The trigger is designed to operate in two stages or levels. The first level operates between beam crossings which now occur every 7 μs. The level one trigger does not cause any deadtime. The second level trigger operates on events which pass the first level trigger. More detailed and accurate processing of the events occur during level two. The difference between level one and level two is that level one incurs no deadtime and level

two does. The same signals and mostly the same hardware are used by both the level one and level two trigger.

The trigger operates on the calorimetry information by adding the energy from different calorimeter trigger towers together. The sum is made over all towers with energy greater than a single tower threshold for level one. The single tower threshold is typically set at 1 GeV for a jet trigger and 2–5 GeV for an electron trigger. If the total energy is greater than the total threshold, a level one calorimetry trigger is generated. There are separate total thresholds for electromagnetic, hadronic, and total energy. There are four independent sets of analog summing circuits (summers) which can operate with different single tower thresholds and total thresholds.

During level two operation the summation of energy is done by clusters. A list of all trigger towers with energy greater than a high seed threshold is loaded into the cluster finder. Then a list of all trigger towers with energy greater than a lower shoulder threshold is loaded into the cluster finder. The cluster finder isolates one cluster which starts at a seed tower and consists of adjacent connected shoulder towers. The energy of the cluster is summed over the trigger towers contained in the cluster. In addition to the total energy, information on the position in ϕ and η, the width in ϕ and η, the number of trigger towers in the cluster, and the identification of the starting tower in the cluster is generated. The presence of a stiff track or muon associated with the cluster is also indicated. This list of information about clusters is used by the level two processors to accept or reject the event at level two time.

The trigger is connected to the data acquisition system through the trigger supervisor [3]. When the detector is running, the trigger supervisor generates the timing signals, clear-and-strobes, which clear the previous crossing information from the front-end electronics and latch the information from the current crossing. If the trigger system generates a level 1 accept the trigger supervisor will inhibit the reset of the front-end sample and holds. The trigger system will then run the level 2 analysis. If level 2 rejects the event the trigger supervisor will start the front-end resetting and sampling. If level 2 accepts the event the trigger supervisor will initiate a full readout of the detector. When the readout is finished the trigger supervisor will again enable the detector.

3. Description of the trigger hardware

The trigger system is built on about 300 Fastbus boards housed in 26 Fastbus crates [4]. Fastbus is used in the trigger for testing, downloading and event readout. The trigger can be tested by loading simulated events into DACs at the front and propagating the signals through the rest of the system. The loading of the DACs and readout of their effects is done via Fastbus. Trigger gains, offsets, and programs are also loaded through Fastbus. This operation takes place during the initialization of the detector and the data remains unchanged during a run. Finally the results of a trigger decision are read out with an event via Fastbus. During the operation of the trigger Fastbus activity is locked out; the actual processing of trigger signals and trigger decisions take place via dedicated connections and special backplanes. The Fastbus interface and protocol are peripheral to the operation of the trigger and are not discussed in detail here [5].

A block diagram of the trigger system is shown in fig. 1. Signals from the detector are received and processed by the receive and weight (RAW) and compare and sum (CAS) cards. The processing is controlled by the timing control and by the cluster finder. The track processor and muon logic can also control the analog processing in order to match muons and straight tracks to energy depositions. The output of RAW and CAS is digitized by the crate sum (CS). The output of the crate sum is split by the interceptor (not shown) to the level one sum for the level one decision, and the list maker for the level two processing. The output of the list maker is a compact list (three 64 bit words) which describe each energy cluster or stiff track or muon. This list is used by the level two processors to make the level two trigger decision.

The trigger system communicates the decisions to the trigger supervisor via a programmable device FRED (the source of the acronym has been lost). Inputs from other level one detector systems, such as the beam–beam counters and the silicon hodoscopes enter into the trigger system through FRED. The connections between FRED and the trigger supervisor are via a set of crosspoints. This allows different parts of the detector to run in different partitions, each with its own trigger, for tests. When the detector is run as a whole for data collection there is only one partition. We now will describe each of the components of the trigger system in detail.

3.1. Trigger cables and the tubesum

Front-end electronics (RABBIT electronics) [6], consisting of charge integrating amplifiers, are located on the detector in the collision hall. Differential analog signals are sent upstairs to the trigger counting room via 200 ft lengths of specially designed cable. The signals from the RABBIT electronics are series terminated at the detector end in 49.9 Ω resistors for both wires of a pair. This configuration is chosen to produce the best possible settling time of signals at the trigger end of the cable in accordance with the design of the cable. Ap-

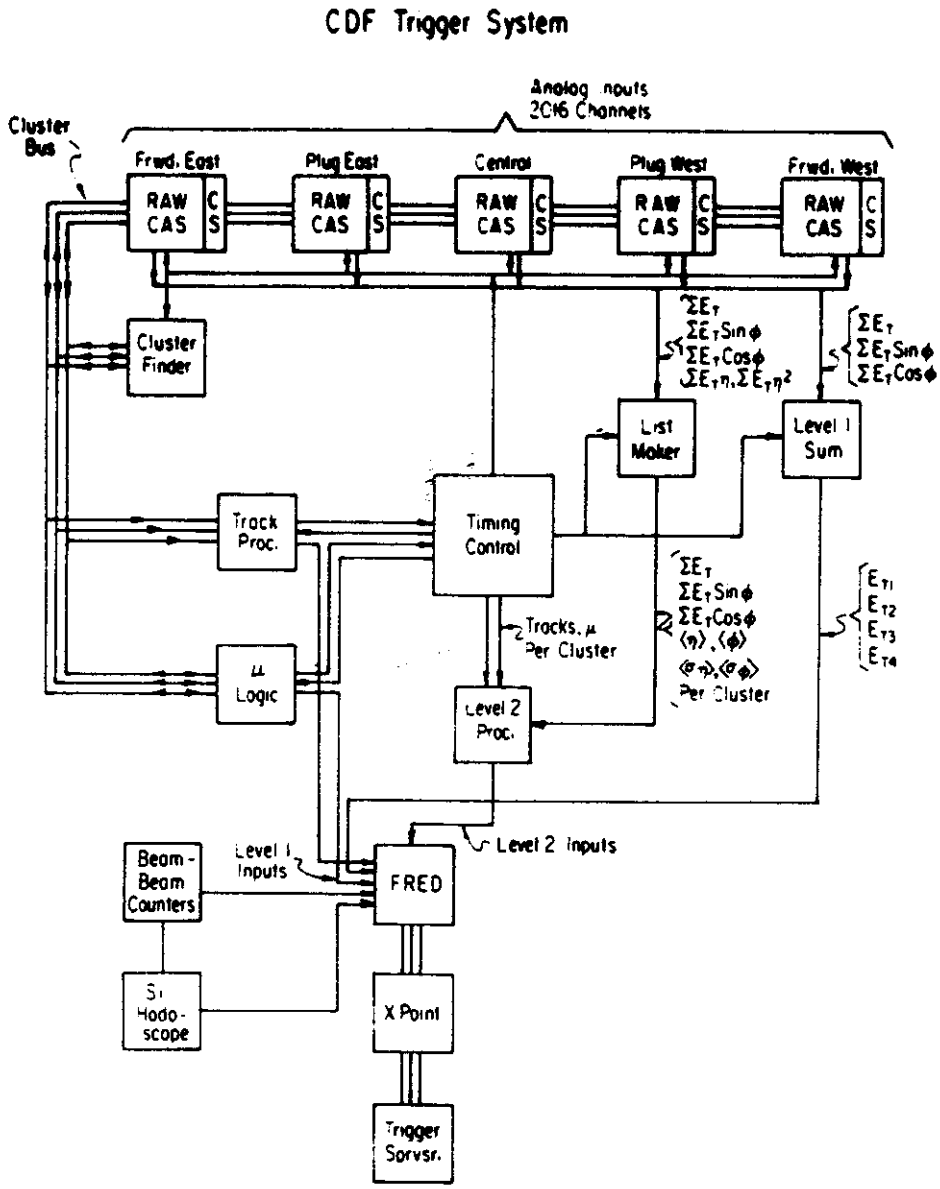

Fig. 1. A block diagram of the CDF Level 1 and Level 2 trigger system.

proximately 60 dB of common mode noise rejection for signals of frequencies up to 20 kHz is achieved with this design.

Two different varieties of the cable exist, one for the scintillator based calorimeters, which are viewed by photomultiplier tubes, and one for the gas proportional chamber calorimeters. The cables from the scintillator calorimeters, covering the central region from $\eta = -1.0$ to $\eta = +1.0$, consist of four shielded twisted pairs with a drain wire having electrical contact with the shield. The four shields are mylar–aluminum laminated and are insulated from each other. The insulation on individual wires is foamed polypropylene. The four shielded twisted pairs are themselves shielded with aluminized mylar with a drain wire. The outer shield is wired to the ground at both the detector and trigger ends, while the individual twisted pair shields are connected to ground only at the detector end. These inner layers act as a Faraday shield, while the outer shield relates the grounds of the signals at each end. The cable has an impedance of 100 Ω and a capacitance of 12.5 pF/ft. The propagation velocity is $0.78c$.

The central calorimeter consists of projective towers of 15° width in ϕ and a width of 0.1 in pseudo-rapidity, η. Each of these towers is viewed by two photomultipliers. This projective geometry is preserved in the

trigger, but to reduce the number of signals, four photomultiplier signals are summed together to produce logical trigger towers with a width of 0.2 in η and 15° in ϕ. This summation is done on a Fastbus card called the tubesum where sets of four analog inputs are summed in high input impedance operational amplifiers. The output impedance of the op-amps is matched to the output cable using 0.1% resistors. The speed and settling time of the summing circuit are much faster than that of the input signal. The tubesum cards as presently implemented have no intelligence, taking just ±15 V power from the Fastbus crate. We have left room to make, if necessary in the future, an intelligent tubesum card where such things as a comparison of the pulse heights between two tubes can be made in order to compensate for nonuniformities in the response of the calorimeters.

The signals reaching the trigger system at the end of the 200 ft cables have a risetime of approximately 500 ns (10%–90%). About 2 μs after a beam–beam interaction, signals at the trigger end of the cables have settled to within 1% of their final values. These signals have a long decay time (up to several minutes) which allows them to be considered as essentially DC. The gain of the front end electronics has been adjusted so that, for central calorimeters, a 100 GeV energy deposition in the center of a tower gives −1 V out of the tubesum.

The gas calorimeters, which have finer azimuthal segmentation, are also summed into logical trigger towers of $\Delta\phi = 15°$ and $\Delta\eta = 0.2$. In this case, however, the summation is done at the detector on the front end amplifier cards. After summation into trigger towers, the signals are sent to the trigger counting room via cables similar to those used for the central calorimeters, but with just one twisted pair per cable. Gas gains are adjusted such that a 50 GeV transverse energy deposition produces −1 V at the trigger. The discrepancy between central and gas calorimeter gains is compensated for in the trigger system. This compensation is performed in the receive and weight (RAW) cards which form one of the major components of the analog front end of the trigger system.

3.2. Receive and weight

The RAW board is the entry point into the processing electronics of the CDF trigger. Signals from the central calorimeters are relayed from the tubesum to RAW over cables of the same construction as the cables from the detector to the tubesum. Signals from the gas calorimeters go directly from the detector into RAW.

The RAW cards are distributed among the ten analog Fastbus crates of the trigger system which they share with the compare and sum (CAS) and crate sum cards. Each RAW card contains 24 channels, from a single $\Delta\eta = 0.2$ slice of either electromagnetic or hadronic calorimeter. The 24 channels correspond to the 24 different ϕ values for a given η slice. The calorimeter signals are received in RAW by a high input impedance, balanced, differential amplifier with a gain of minus three. The output of this amplifier is input to a dual multiplying DAC with output

$$V_{out} = 0.5[(V_{in}W)/256] + [(0.5B)/256],$$

where W is a weighting factor between 0 and 255, and B is a bias between 0 and 255. The weighting factor accommodates gain variations and generates the sin θ factor needed for converting E to E_t for the central calorimeters. The adjustable bias is used to compensate for calorimeter amplifier pedestals. It is at this stage that the compensation for the gas gain is made by reducing the weight W by a factor of two. The output of the dual multiplying DAC is fed into a noninverting amplifier with a gain of four, and then to an emitter-follower. The output of the final RAW amplifier stage is then relayed across a short jumper to the RAW companion card, CAS. The DAC bias constant, 0.5 V, can be changed to 3 V so that with $W = 0$ the bias can be used as a source of simulated inputs for trigger testing.

The RAW board has an 8 bit high speed DAC that can be controlled either by Fastbus or by the crate sum. The output of the fast DAC is a differential current which is sent to CAS where it is converted to a voltage and used as the reference in the comparators. RAW also contains correction circuits to maintain linearity and full scale range for the fast DAC.

The digital section of the RAW card includes the Fastbus protocol for both RAW and CAS, shadow memory that holds the digital input values for the multiplying DACs (W & B), and registers for CAS control.

3.3. Compare and sum

Each CAS card has 24 channels in a one to one correspondence to the 24 channels on the companion RAW card. During the level 1 cycle, the function of the CAS card is to sum all towers from a single RAW card that are above a programmable threshold. CAS does not have Fastbus protocol, only connections to the Fastbus address and data lines (AD lines). All controlling strobes are generated on RAW. If the cable connecting a RAW/CAS pair is removed, CAS goes to a quiescent state with all signals removed from the AD lines.

Each analog signal from RAW is delivered to a set of analog switches, and to the positive input of a comparator. The other input to the comparator is the reference voltage produced by the fast DAC and RAW. When a particular analog signal is over threshold, the corresponding comparator output is loaded into a sum register. The state of this register controls the analog switch matrix, directing the tower signals into summing amplifiers. Three different sums are performed for those

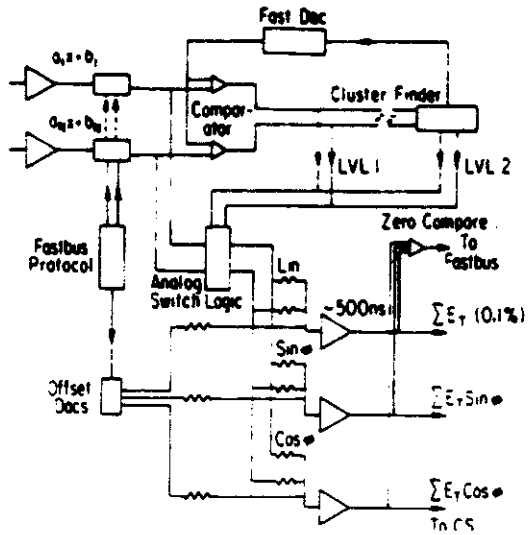

Fig. 2. A simplified schematic showing the operation of the Receive and Weight and Compare and Sum boards.

towers above threshold, a linear sum, a sum weighted by sin ϕ, and a sum weighted by cos ϕ. It takes approximately 500 ns for the analog sum signals to settle to 0.1% accuracy. At level 1 time, these sums are performed to an accuracy of about 1% (determined by the settling time of the signals from the front end electronics). There are four sets of sum circuits on each channel of CAS, so that four different tower thresholds may be loaded in parallel (at level 2 time, this parallelism facilitates high speed operation).

Each of the twelve sum circuits is monitored by a zero detection circuit. The outputs of the twelve zero detection circuits are available as a Fastbus register. There are also twelve eight-bit DACs, one per sum circuit. The output of the DAC is used as a bias for the corresponding sum circuit. These devices allow for correction of input offset bias by ramping the offset DAC and monitoring the state of the zero crossing comparator.

A block diagram outlining the various functions of the RAW and CAS cards is shown in fig. 2.

A register known as the inclusion register is used as a mask to either inhibit, allow, or force participation of specific towers in the summation. This register has one bit for each of the 24 analog channels. If the inclusion register is enabled, then only those channels whose inclusion register bit is set to one will be permitted to activate a comparator. If inclusion register negation is in effect, the converse is true. This function allows masking of bad channels in the calorimeter or in the trigger. The inclusion register can also be loaded into a sum register thereby forcing a channel to be summed.

The output of any CAS register can be gated onto the Fastbus AD lines under the control of the Fastbus protocol circuits located on RAW. In addition, the four sum registers, the inclusion register and the cluster finder bus can all be loaded via Fastbus.

3.4. Cluster finder

The level 2 decision begins with the interaction between CAS and the cluster finder board. During level 1, the outputs of the comparators on CAS are loaded directly into the sum registers. During level 2 these outputs are first loaded into the cluster finder. The cluster finder processes the data and returns a set of towers corresponding to one cluster to CAS where it will then be loaded into a sum register. This procedure causes CAS to create sums for individual clusters of energy in the calorimeters.

The procedure for finding calorimeter clusters is as follows. The threshold value loaded into the fast DAC on RAW is a decreasing ramp. The comparator threshold starts at a high value (e.g. 10 GeV) and begins to decrease until one or more calorimeter towers are above threshold, at which point the ramp stops and the outputs of the comparators are gated onto a 1008 bit wide bus (24 × 42, the logical OR of the comparator outputs from the electromagnetic and hadronic crates), the cluster bus, and transferred to the cluster finder as seed values. A second, low threshold (e.g. 1 GeV) is then loaded into the fast DAC, and the towers above this threshold are loaded into the cluster finder as shoulder towers. At this point CAS ceases driving the cluster bus. The cluster finder asserts the η addresses of all seeds and the cluster control card selects the smallest η value and enables the cluster finder to assert the ϕ addresses of all seeds of the selected η. The cluster control card then selects the smallest ϕ value and enables the tower with the selected η and ϕ values to turn on. The selected tower sends a signal to its four nearest neighbors (the diagonal neighbors with different η and different ϕ values are not included) instructing them to turn on if they are above the shoulder threshold. The newly selected towers send signals to their nearest neighbors and so on until no more contiguous towers are found. A bit map of all towers in the cluster is then sent back over the cluster bus to CAS where it is loaded into a sum register. The process is repeated at a cycle time of about 150 ns until no new seed towers exist. At this time the high threshold may be lowered and the process repeated. Once a tower is included in a cluster, it is prohibited from being included in any of the subsequent clusters.

During the processing of clusters, the track finders are monitoring the cluster bus. When a cluster bit corresponding to the coordinates of a stiff track is turned on, 5 bits are sent from the track finder interface (built by University of Illinois at Urbana) to the interceptor. One bit indicates the existence of a stiff track,

and 4 bits provide its momentum. These bits are included in a 64 bit word which is sent to the level 2 processors.

3.5. Crate sum

The transition between the analog portion of the trigger and the digital portion takes place in the crate sum. In each analog crate there is one set of crate sum boards which receive the analog sums E_t, $E_t \sin\phi$ and $E_t \cos\phi$ from each CAS board, and perform a further stage of analog summing to produce complete sums at the crate level. In addition to these sums, the crate sum uses hardwired weighting factors corresponding to the mean pseudo-rapidity, η, of each CAS card to produce the sums $E_t\eta$ and $E_t\eta^2$. The pseudo-rapidity weighted sums are used only during level 2. Each analog sum is digitized in an 8-bit flash ADC (FADC) and sent, for level 1, to the level 1 sum board. There are four sets of identical analog summing circuits in the crate sum, corresponding to the four sets of summing circuits on each CAS card.

The analog section of the crate sum is contained on two boards. The first board uses high speed summing operational amplifier circuitry to produce the four $E_t \sin\phi$ and $E_t \cos\phi$ sums from the analog signals coming from the ten CAS boards in the crate. Each of these sums is then digitized in a FADC upon command from the timing control board. The second analog crate sum board uses the E_t signals from the CAS boards to produce the E_t, $E_t(\eta - \eta_0)$, and $E_t(\eta - \eta_0)^2$ sums, where η_0 is the mean rapidity in that crate. The sums about the mean are taken in order to optimize the resolution of the FADCs. The 120 analog input signals which come from the CAS cards to the crate sum are contained in a specially designed fourteen layer auxiliary backplane. The digital output from the four sets of sum circuits passes through a multiplexer, with the selected set passing to the digital crate sum board.

The digital board receives one set of E_t, $E_t \sin\phi$, $E_t \cos\phi$, $E_t(\eta - \eta_0)$ and $E_t(\eta - \eta_0)^2$ sums. It performs the digital arithmetic necessary to produce 2's-complement values of E_t, $E_t \sin\phi$, $E_t \cos\phi$, $E_t\eta$, and $E_t\eta^2$. This board also produces N, the number of calorimeter towers which are part of a level 2 cluster. As an option, if N is zero the other 5 quantities can be forced to zero to help suppress noise. The Fastbus protocol and all of the registers for the crate sum reside on this board. Finally, all RAW, CAS, and crate sum control signals which come from the timing control, pass through the digital crate sum board. Control signals for the RAW/CAS pairs are shipped out on the special backplane.

3.6. Interceptor

The digitized output from the crate sum is required by the level one sum and by the list maker. The interceptor receives two quantities from two crate sums, one hadronic and one electromagnetic. The data is reorganized and transmitted to the level one sum and listmaker via separate cables. The interceptor uses 1K of RAM to record the information from the crate sum. The interceptor also receives the η and ϕ index of the cluster seed tower from the cluster finder and information from the tracking and muon system.

The interceptor can operate in two modes. In the first mode the data from the crate sum is recorded in memory and simultaneously transmitted to the list maker and level one sum. In the second mode data input to the interceptor is first stored in memory and then later recalled from memory and transmitted to the list maker. This is necessary because not all of the quantities corresponding to a cluster are available simultaneously, yet the cluster memory requires that all information be latched at the same time. For example, the η and ϕ coordinates of the seed tower from the cluster finder are valid at the time the cluster is found. By the time the E_t of the first cluster is digitized by the crate sum the cluster finder is finding the fifth cluster.

The interceptor has two pointers to its memory. One is used for writing information to its memory as it becomes available from the separate parts of the trigger. The second is used to read out from its memory all data corresponding to a single cluster simultaneously.

The interceptor is also used for testing the trigger system. Crate sum data from simulated events may be stored in the interceptor and played out at full speed. All systems downstream will be unable to distinguish whether the data are real or if they are from memory.

3.7. Listmaker

The listmaker consists of three different types of boards. Together they perform a variety of arithmetic functions on digital values received from the crate sums to produce a list of properties of the clusters found by the cluster finder. The list consists of two 64 bit words per cluster (a third word has its origin in the interceptor), one for electromagnetic energy quantities and one for total energy quantities. The contents of the two words includes 10 bits each of E_t, $E_t \sin\phi$, and $E_t \cos\phi$, 8 bits each of $\langle\eta\rangle$ and the width of the cluster is η, σ_η, 7 bits of $\langle\phi\rangle$, and 8 bits of σ_ϕ. In the event that a calorimeter cluster spans the boundary between crates, the first three quantities listed will be different from that produced by any single crate sum module.

The first of the three listmaker boards, the sum board, receives the 12 bit quantities output by the crate sum. There is one sum board for each of the six quantities, and each board receives the outputs of five electromagnetic and five hadronic crate sums. These boards sum over the ten crates to produce a 12 bit electromagnetic energy sum and a 12 bit total energy sum. A

pipeline latch at the output stage of the sum board is strobed by the timing control. The 12 bit sum for N is sent to the interceptor for inclusion in the third word of the list. The remaining five 12 bit sums are sent to the second of the listmaker boards, the multiplier board, consisting of an array of 4K RAMs and an array of high speed multipliers. There are two multiplier boards, one operating on electromagnetic energy sums, and one operating on total energy sums. The 12 bit sum E_t forms the address to the RAMs whose output is a 12 bit representation of $1/E_t$. Four sets of multipliers are used to form the products of $1/E_t$ with each of the four quantities $E_t \sin\phi$, $E_t \cos\phi$, $E_t\eta$ and $E_t\eta^2$. The outputs of the multipliers, $\langle \sin\phi \rangle$, $\langle \cos\phi \rangle$, $\langle \eta \rangle$ and $\langle \eta^2 \rangle$ are sent to the last of the three boards, the RAM board. Once again there is one RAM board operating on the electromagnetic energy quantities and one on the total energy quantities. Here a number of functions are performed, primarily through the use of look-up tables stored in RAMs, and the last three quantities needed, $\langle \phi \rangle$, σ_ϕ and σ_η are calculated from:

$$\langle \phi \rangle = \sin^{-1}(\langle \sin\phi \rangle) \quad \text{if } |\langle \cos\phi \rangle| > |\langle \sin\phi \rangle| \quad \text{or } \cos^{-1}(\langle \cos\phi \rangle) \quad \text{otherwise}$$

$$\sigma_\phi = \sqrt{1 - \langle \sin\phi \rangle^2 - \langle \cos\phi \rangle^2}\,,$$

$$\sigma_\eta = \sqrt{\langle \eta^2 \rangle - \langle \eta \rangle^2}\,.$$

The five listmaker quantities (excluding N) are then latched by a strobe from the timing control at the output stage of the RAM board for use by the level 2 processors.

3.8. Other level 2 triggers

When the interaction between the cluster finder and CAS finishes, the muon systems take over the cluster bus, turning on bits corresponding to the η and ϕ locations of muon candidates. For central muons, these candidates are "golden muons", i.e. those muon candidates with CTC stiff tracks directed at them. The map of all muons found is loaded into the cluster finder from the cluster bus. The cluster finder will then select one muon at a time and assert the corresponding bit on the cluster bus. During this time the muon match box monitors the cluster bus and sends to the interceptor the momentum of each muon as it is selected. The cluster finder will send the η and ϕ values for the selected muon to the interceptor where it will be included in the third of the three 64 bit words to be sent to the level 2 processors. As each bit on the cluster bus is turned on, the CAS – crate sum – listmaker processing proceeds as usual so that the first two words of the list received by the level 2 processors contain information regarding energy deposition in the calorimeter by the muon candidates.

3.9. Cluster memory

The list of calorimeter clusters, isolated muons and total event energy is sent to the level two processors in the form of three 64 bit words. The first two words come from the listmaker representing electromagnetic and total energy. The third word comes from the interceptors and timing control and contains information from the cluster finder, the muon systems, the track finder, and control codes. The third word contains a 4 bit origin code, an 8 bit field containing the number of towers in a cluster, the ϕ and η seed address in 11 bits, and 4 bits of momentum information from the track finder.

The cluster memory module receives one 64 bit word via the front panel and stores it in a 1K by 64 bit memory. The memory can be accessed either by Fastbus or directly by the level two processor via the auxillary backplane.

The auxillary backplane, the processor bus, supports a multimaster single crate protocol invented for use by the level 2 processing system [7]. Data transfers between two modules, a source specified by a 22 bit source address, and a destination specified by a 22 bit destination address occur under control of a processor bus master. Data is transferred in 64 bit words at rates up to 1 transfer every 150 ns, including master arbitration.

The cluster memory can act as either a source or destination on the processor bus. When a cluster is written to the three cluster memory modules, one for each 64 bit word, it is then read out onto the processor bus, one word at a time, and written to several special processing modules, the mercury modules. This allows processing of the cluster list to proceed as the cluster list is being constructed.

3.10. Level 2 processor

The level two processors control the processing and decision making for the level two trigger. There can be up to 6 processors running, each identical in hardware but operating with different programs. The processor is built on two Fastbus boards. The first board, the sequencer, contains the memory for the 64 bit microcode and the logic to fetch and execute instructions. Eighteen instructions controlling execution flow, such as branch on condition, are implemented. Five bits of microcode specify the instruction, 14 specify the next address for a jump instruction, six specify the condition code for conditional branches, and 37 are used by the processor board. The second board, the processor board, contains an ALU, shifter, counter, scratch memory, and processor bus interfaces. The processing elements are organized as registers on two busses, a 10 bit bus for control and a 32 bit bus for data. Each microinstruction specifies the six bit address of the source and destination registers on

both busses. One of the 10 bit source registers is a field in microcode used for loading constants. The level two processor executes an instruction every 40 ns.

The level two processors can either work directly on the data in the cluster memory, extracting the fields of interest, or can recall the results of calculations from the mercury modules and compare them to thresholds. The processors communicate the level two rejects or accepts to FRED.

3.11. Mercury modules

There are currently four mercury modules, each designed to calculate a specific quantity of interest. The mercury modules are processor bus slaves and can act as either a source or destination. The mercury modules do not have any Fastbus interface and must be loaded and read through the level two processor.

The mercury ET module sums the total clustered energy and counts the number of clusters whose energies are above a predefined threshold. This is used, for example, in a two or three jet trigger where each jet is required to be above an energy threshold.

The mercury EL module operates on electromagnetic energy. This is used to select electrons or photons using the cluster width and ratio of electromagnetic to total energy. In addition, the electron is identified by the presence of a high P_T track pointing to the cluster.

The mercury MU module selects muon candidates. The information from the muon system is used to identify the ϕ and η coordinates of a muon. The energy deposition in the calorimeter at the same η and ϕ coordinates is used to identify isolated muons. Muons can be selected based on their momentum. This module also calculates the magnitude of missing ET.

The fourth mercury module, mercury L1, is used to record the level one information. This is used by the level two processors to coordinate level one and level two decisions. For example if the level one trigger was generated by a prescaled minimum bias trigger, level two should not reject it if there is not sufficient energy deposition.

The number of mercury modules can be increased, as the need arises, up to the physical constraints of a Fastbus crate. Since the processor bus cannot communicate between segments. Currently 16 out of the 26 Fastbus slots are occupied.

3.12. Timing control

The synchronization and operation of the trigger is carried out by the timing control. The timing control receives a reference time mark from the master clock and an enable from FRED. When these two signals are present the level one sequence starts. At the end of level one, if there is a level one accept, the timing control will start the level two sequence.

The rest of the trigger system was designed such that modules perform specific actions based upon control signals received via dedicated cables from the timing control. There is no handshaking of these signals, and in general only data is passed between modules. About 300 control signals are needed to operate the trigger.

The timing control consists of two types of boards, a single master and fifteen slaves. The timing control master is physically the same type of board as the level two processor sequencer, with different jumpers. The lower 12 bits of microcode, instead of controlling the level 2 processor, specify a dwell time of from 40 to 81940 ns. The instruction set, condition branch code selection, and jump address fields are identical. As the sequencer executes each instruction the address of the instruction is bussed to the slave modules.

The slave modules use this address to fetch a 32 bit instruction from their memories. The various bits and fields of the slaves instruction are transmitted, via an on board patch area, through front panel connectors to the various trigger modules. Each slave can receive up to 8 signals and present them to the timing control master for use in condition branches. The multiplexing is controlled by the 6 bit condition control field. The slave modules can be configured for each specific application through the patch area. Glitches are prevented by following the memory with an instruction latch. The timing control is programmed by specifying, for each instruction, which control signals are to be asserted or cleared and the amount of time to wait until the next instruction. Since the timing control also contains such information as comparator thresholds a separate program is created and downloaded at the beginning of each run.

3.13. FRED

The communication between the trigger system and the data acquisition system is through FRED. The detailed protocol between FRED and the trigger supervisor (level 1 query, and level 1 accept followed by level 2 accept or reject) must follow a well defined sequence. Any deviation from the sequence forces the trigger supervisor into an error state and causes data acquisition to cease. FRED provides 12 level 1 and 6 level 2 protected input ports for user connection.

There are 12 input ports for level one triggers. These 12 ports form the address lines for a 4K by 4 bit memory. If a particular port or combination of ports is required to generate a trigger, a logic 1 will be placed at initialization time in the memory location corresponding to the appropriate address. Each of the four bits is further conditioned by a rate limiting circuit which is

used to limit a particular trigger to a maximum rate, if enabled.

FRED also coordinates up to six level 2 processors. Each processor may be marked as ON, OFF or VETO. A level 2 accept is generated when any of the ON processors generate an accept and all of the VETO processors generate an accept. A level 2 reject is generated when all of the ON processors generate rejects or any of the VETO processors generate a reject.

A simple version of FRED, autonomous FRED, exists for generating simple triggers, e.g. calibration.

The level 1 signals used by FRED to determine a level 1 accept were, for this last run:

A) Four calorimetry triggers with different threshold.
B) Two beam-beam counter triggers, one for the east and one for the west side.
C) Central muon from the central muon chamber.
D) Forward muon from the muon toroids.
E) Forward silicon from small angle silicon detectors.
F) Central high P_t track from the track processors.

Table 1
Example of physics table

```
!
!       Physics table creation date: 23-MAR-1987 21 40:00.11
!
!       FILTER A IS FOR JETS, STT = 1, TOTAL = 30
!
!       FILTER B IS FOR ELECTRONS, STT = 5, TOTAL = 15, EM ONLY
!
!       FILTER C IS FOR MUONS, RATE LIMITED TO 0.15 HERTZ
!
!       FILTER D IS FOR MIN BIAS, RATE LIMITED TO 0.07 HERTZ
!
BEGIN_FILTER    LEVEL1A
BEGIN_TRIGGER   TRIGGER_0001
        OPTION  BBC_WEST
        OPTION  BBC_EAST
        OPTION  A_CAL_LEVEL1
                PARAMETER EM_TOWER_THRESHOLD > (1.00)GEV
                PARAMETER HADRONIC_TOWER_THRESHOLD > (1.00)GEV
                CUT EM_ET > (30.00)GEV
                CUT HADRONIC_ET > (30.00)GEV
                CUT TOTAL_ET > (30.00)GEV
END_TRIGGER     TRIGGER_0001
END_FILTER      LEVEL1A
!
BEGIN_FILTER    LEVEL1B
BEGIN_TRIGGER   TRIGGER_0001
        OPTION  BBC_WEST
        OPTION  BBC_EAST
        OPTION  B_CAL_LEVEL1
                PARAMETER EM_TOWER_THRESHOLD > (5.00)GEV
                PARAMETER HADRONIC_TOWER_THRESHOLD > (51.00)GEV
                CUT EM_ET > (15.00)GEV
                CUT HADRONIC_ET > (127.00)GEV
                CUT TOTAL_ET > (127.00)GEV
END_TRIGGER     TRIGGER_0001
END_FILTER      LEVEL1B
!
```

Table 1 (continued)

```
BEGIN_FILTER    LEVEL1C
        GLOBAL_OPTION   LEVEL1_RATE_LIMIT
                PARAMETER BURST_COUNT = (1.00)
                PARAMETER BURST_LOAD_RATE = (0.15)HZ
BEGIN_TRIGGER   TRIGGER_0001
        OPTION  BBC_WEST
        OPTION  BBC_EAST
        OPTION  CMU_LEVEL1
                CUT CMU_L1_PT > (5.00)GEV
        OPTION  CFT_LEVEL1
END_TRIGGER     TRIGGER_0001
BEGIN_TRIGGER   TRIGGER_0002
        OPTION  BBC_WEST
        OPTION  BBC_EAST
        OPTION  FMU_LEVEL1
END_TRIGGER     TRIGGER_0002
END_FILTER      LEVEL1C
!
BEGIN_FILTER    LEVEL1D
        GLOBAL_OPTION   LEVEL1_RATE_LIMIT
                PARAMETER BURST_COUNT = (1.00)
                PARAMETER BURST_LOAD_RATE = (0.075)HZ
BEGIN_TRIGGER   TRIGGER_0001
        OPTION  BBC_WEST
        OPTION  BBC_EAST
END_TRIGGER     TRIGGER_0001
END_FILTER      LEVEL1D
```

4. Software

The trigger system, in order to be versatile, is highly programmable. The timing control which specifies how the various parts of the trigger operate, must be programmed for each run. The program for the level 2 processors must also change as the trigger requirements change. The job of the software required to operate the trigger is to translate the desires of the physicist running the experiment into the programs and tables that are downloaded. To accomplish this we have devised a system of 'OPTION TABLES' and 'PHYSICS TABLES'. The option table specifies all of the objects which can be used in the trigger along with the ranges of cuts and parameters describing this object. Options can be selected and put into a physics table. The physics table displays the AND–OR structure of the options and specifies the values of cuts and parameters. This may be best explained by the example in table 1.

This physics table has four filters for level one, corresponding to the four sets of level one lookup RAM and FRED. The first filter requires that the total transverse energy in the detector be greater than 30 GeV, summed over all towers with more than 1 GeV. This is in coincidence with a beam–beam interaction. The second filter is for electrons. Here the requirement is that EM transverse energy be greater than 15 GeV for EM

towers above 5 GeV. Again there is a beam–beam counter requirement.

The third filter contains two triggers. A level 1 accept is generated when any one of the four filters is accepted. A filter is passed if any one of the triggers it contains is accepted. A trigger is passed only if all of the conditions specified by it are met. In this case we want to accept their forward muons or central muons with $P_t > 5$ GeV. This trigger is limited to a maximum rate of 0.15 Hz. The fourth trigger is monitoring the detector. This is a minimum bias trigger requiring only a beam–beam interaction. This is rate limited to 0.075 Hz.

We have written the software which can parse these physics tables and generate the programs to be downloaded into the hardware. A compiled version of each physics table is maintained to expedite downloading.

5. Conclusion

We have designed and built a sophisticated programmable trigger system. The system is flexible in that event criteria can be specified on a run by run basis. It is also expandable in that more types of level one inputs may be added to FRED and additional mercury modules may be added to the level 2 processor system. During the 1987 run the collider achieved a luminosity in excess of 10^{29} cm^{-2} s^{-1}. The trigger was able to maintain a rate to tape of 1 Hz. With the addition of level 2 for the next run, operation at 10^{30} cm^{-2} s^{-1} without loss of interesting physics processes will continue.

References

[1] H. Jensen et al., these Proceedings (Advances in Experimental Methods for Colliding Beam Physics) Nucl. Instr. and Meth. A265 (1988) 186.

[2] R. Wagner et al., these Proceedings (Advances in Experimental Methods for Colliding Beam Physics) Nucl. Instr. and Meth. A265 (1988) 1.

[3] S. Galleotti, H. Gonzalez, D. Hanssen, C. Horvath, K. Konigsfel, D. Passuello, L. Ristori, R. Vidal, Trigger Supervisor Operational Description, CDF Report No. 451, unpublished.

[4] Fastbus Modular High Speed Data Acquisition and Control System, US NIM Committee (1983) DOE/ER-0189.

[5] D. Amidei et al., IEEE Trans. Nucl. Sci. NS-33 (1) (1986) 817.

[6] G. Drake, T.F. Droege, C.A. Nelson, K.J. Turner and T.K. Ohska, IEEE Trans. Nucl. Sci. NS-33 (1) (1986) 92.

[7] M. Campbell, The Processor Bus, Trigger group note 47 (1986), unpublished.

APPENDIX B

DRIFT TUBE SYNCHRONIZERS

J. Chapman
University of Michigan

UM – HE – 89 – 10
June 21, 1989

Drift Tube Synchronizers

J. Chapman

University of Michigan, Ann Arbor, Michigan

Submitted to Nuclear Instruments and Methods

ABSTRACT

Two rather simple circuits are presented that delay the signals from drift tubes so that an output appears at the maximum drift time of the tubes independent of the position of the track within the tubes. The first version is designed to sense high momentum tracks in multi-layered straw tubes where approximate normal incidence is assumed. The second version is designed to accept angled track signals from a triad of tubes. Software simulations of both circuits indicate that the technique can prove very effective for fast coincidence between tracking layers or between tracking and calorimetry.

Introduction

The SSC interaction rate of $10^8/s$ and the high track multiplicity make the development of triggers a major challenge. This high rate environment has been presented in two papers specifically for straw chambers.[1][2] It appears from these studies that offline tracking with small tubes can be effective even at the full SSC luminosity. The problem remains as to how one can assure that the events to be tracked are accepted by the trigger logic. In this paper two circuits are presented as possible aids to the triggering problem. The first is motivated by the need to sense segments from high transverse momentum tracks and to determine which collision produced them. This must be done without excessive accidentals from the high occupancy prevalent at the SSC. A superlayer with a depth of eight tubes is considered and shown partly in Figure 1a. For the high momentum case it is assumed that tracks are 10 GeV or greater and have bend angles less than $\pm 0.5°$ at a superlayer 1.6m from the interaction. This assumption is consistent with a solenoidal field of ≤ 0.5T.

A second circuit adopts a similar approach to the problem of generating a trigger signal from the passage of a particle through a triad of drift tubes as illustrated in Figure 1b. The central tube is assumed to be staggered a half cell relative to the outer tubes. As in the superlayer case, the goal is the generation of a pulse that is fixed in time relative to the passage of the particle. In this case only mild angle restrictions are imposed. This second circuit is being considered as a component of a μ trigger. A coincidence of several radially associated triads is one possibility.

Superlayer Segment Finding

The Circuit

The circuit for processing an 8 tube group is shown in Figure 2. The goal of this circuit is to produce a pulse, T_0, a fixed time after the passage of a stiff track through the superlayer. Stiff is defined by the range of track angles, with respect to the normal to the superlayer, that yield hit times satisfying the coincidence requirement of the circuit. This coincidence is needed for random hit suppression. A three out of four coincidence is included as a means of reducing the effects of tube inefficiencies. Analysis of the circuit

that follows will be in terms of the coincidence of the even and odd layers, t_l and t_r respectively. The equations are precise for normal incidence but are only approximations for the range of angles accepted by the coincidence circuit. The simulation will exhibit this as a variation in the timing of T_0.

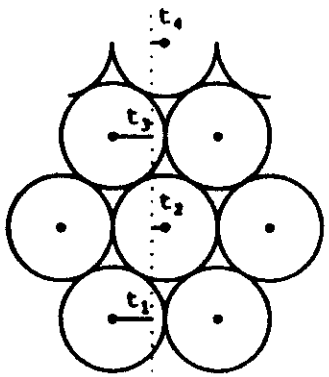

Figure 1a

Superlayer

Figure 1b

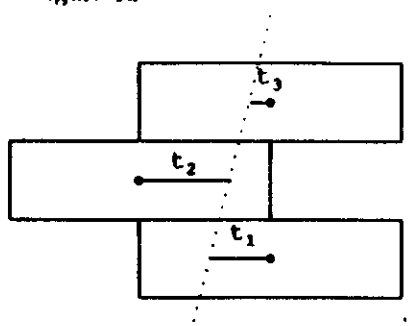

Tube Triad

The behavior of the circuit of Figure 2 is interpreted in the context of the following derivation. For tracks normal to the superlayer, the drift times t_l and t_r of Figure 1a can be related to the radius of the tube, r, according to the simple equation, $t_l + t_r = r/k$. In this equation k is the drift velocity assumed for the moment to be a constant, and r is the radius of the tubes. Charge is taken to arrive at the right wires at time t_r before time t_l. This choice for the ordering is just a matter of labeling and in no way restricts the circuit since inspection of the schematic quickly reveals that the circuit is symmetric with respect to the two inputs. The above equation can be rewritten as,

$$(t_l - t_r) + 2 \times t_r = r/k$$

which leads to the following conclusion. If one waits, starting from the arrival of the left hits, an additional amount of time, t_r, that when scaled by 2 and added to the time difference $t_l - t_r$ equals the maximum drift time, then a total time equal to the maximum drift time will have elapsed from the traversal of the original track. It is this programmed delay, t_r, that is generated by the circuit of Figure 2.

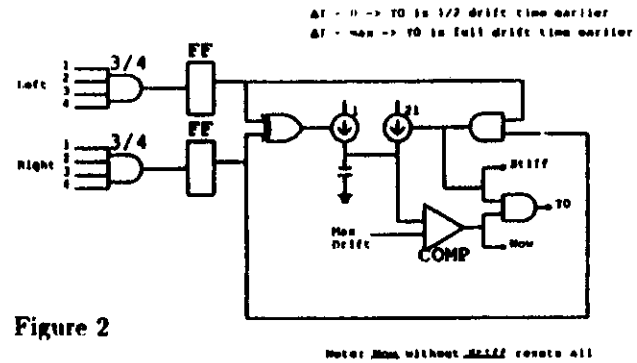

Figure 2

Simplified Stiff Track Finder

The drift time difference is accumulated on a capacitor by integration of a constant current, i, during the time between the arrival of the two pulses. At the time of arrival of the last hit a current of 2i is directed onto the same capacitor. When the accumulated integral has reached the voltage corresponding to the maximum drift time, the comparator outputs the "NOW" signal and a T_0 is generated. A fixed width pulse (not shown) is also generated on the arrival of the "NOW" signal. Its trailing edge resets the flip-flops. This self reset will naturally generate a fixed width T_0. If the integration is triggered and no "STIFF" signal is generated, i.e., both coincidence signals are not produced, the self reset provides a clear for the circuit. The actual circuit implementation will likely contain only current sources that are started by wire hits since one can obtain a current 2i by adding another current i to an existing current i rather than stopping current i and starting current 2i.

Calibration

The reference voltage, MAX DRIFT, is critical to the timing generated by the circuit since it determines the wait time. A built in calibration approach is suggested. In such a scheme two precisely timed calibration pulses would be used. The first would be directed to one or both of the flip-flops of the circuit. The second pulse, timed precisely to the desired generation time for the "NOW" signal, would be compared in timing to the signal

"NOW". If T_0 was late in arriving, the current leading to "NOW" would be incremented. After some number of test pulses the current would reach the value required to synchronize "NOW" to the desired time. If "NOW" was found to arrive early, the current would be decremented.

There are two patterns of auto-calibration possible in the above scheme. Pattern one would trigger both flip-flops at the same time. This pattern would activate only the 2i current and hence adjust it only. A second pattern would trigger only one of the flip-flops and result in the adjustment of the current i. As will be seen later, this auto-calibration at what amounts to the full and half cell drift times can be used to reduce the effects of non-linearities in the time-distance relation for gas tubes.

Simulation

A program to assess the effectiveness of the straw tube circuit has been written and utilized to study the proposed circuit. The program includes the effects of tube inefficiencies and random occupancies in generating the coincidence signals. It includes time-distance non-linearities in the form of a quadratic term. It should be noted that for tracks at angles to the superlayer normal, the circuit behavior is not exact. In addition, the signals input to the circuit must have a specific width if the coincidence is to be realized. Understanding these approximations will be the major utility of the simulation. The goals of the simulation were to determine the:

- Sensitivity of the T_0 timing to the track angle from the normal.
- Efficiency of the circuit for various values of individual tube efficiencies.
- Efficiency of the circuit in the presence of random background hits.
- Sensitivity of the circuit to non-linearities in the time-distance relation.
- Coincidence width that is required to accept tracks at various angles.
- Effectiveness of auto-calibration in reducing the impact of non-linearities.

Results

The response of a superlayer of 4mm diameter tubes was simulated for tracks entering the tubes between adjacent wires in the first two layers. The simulated tracks were given a ±25mr range of angles from the normal to the superlayer. Only tracks passing through

the tubes in patterns that could be expected to activate the electronics were considered. Others were counted and designated as inefficiencies. These geometrical losses are distinct from those due to individual tube inefficiencies in that these geometrical losses would exist even for 100% efficient tubes.

After tracks were determined to be within the active area of the simulated tubes, the drift times were determined according to a form containing a linear and a quadratic term. The relative size of the quadratic was varied from 0 to 40% of the linear term at the radius of the tube. Tube inefficiencies were then simulated by removing the hits within tubes in a completely random way with a frequency that was varied from 0 to 5%. Random hits were then introduced at a rate parameterized by the percentage of tubes with random hits within the drift time. Rates up to 10% were tried. The random hit was ignored if it came later in time than the simulated track hit.

The timing difference of the "critical" coincidence inputs are plotted in Figure 3a for fully efficient linear tubes in the absence of background. The term "critical" implies the timing difference between signals that satisfy the 3 out of 4 coincidence. Pulse widths for the inputs must have a difference greater than the value plotted if the input is to satisfy the coincidence. The distribution terminates abruptly at 10ns. This timing difference between the first and last hit arrival for a track is due to the range of angles assumed for the track. The coincidence width is thus one to one related to the lowest momentum accepted. Figure 3b displays the time distribution for the T_0 output for tracks satisfying a coincidence interval of 10ns. The output distribution does not show a zero width since the variation of track angle interacts with the coincidence circuit to give time jitter in the signal from the synchronizer. The data in Figure 3b is from a circuit with nominal currents of i and 2i. Figure 3c shows the response of the circuit for currents optimized for minimum σ of the distribution including a 20% non-linearity in the time distance relationship. The optimized values of the currents are 0.8i and 1.8i. Figure 3d shows the timing distribution for an assumed typical case where nonlinearity, inefficiency, and random noise have been included. These tube characteristics are described later in the text.

The effect of tube inefficiencies is quite consistent with that predicted from simple probabilities and the 3 out of 4 coincidence of the circuit. The value assumed for the inefficiency of the individual tubes does not noticeably change the timing jitter distribution or the optimum currents. Random hits produce a scatter of T_0 when the coincidence is

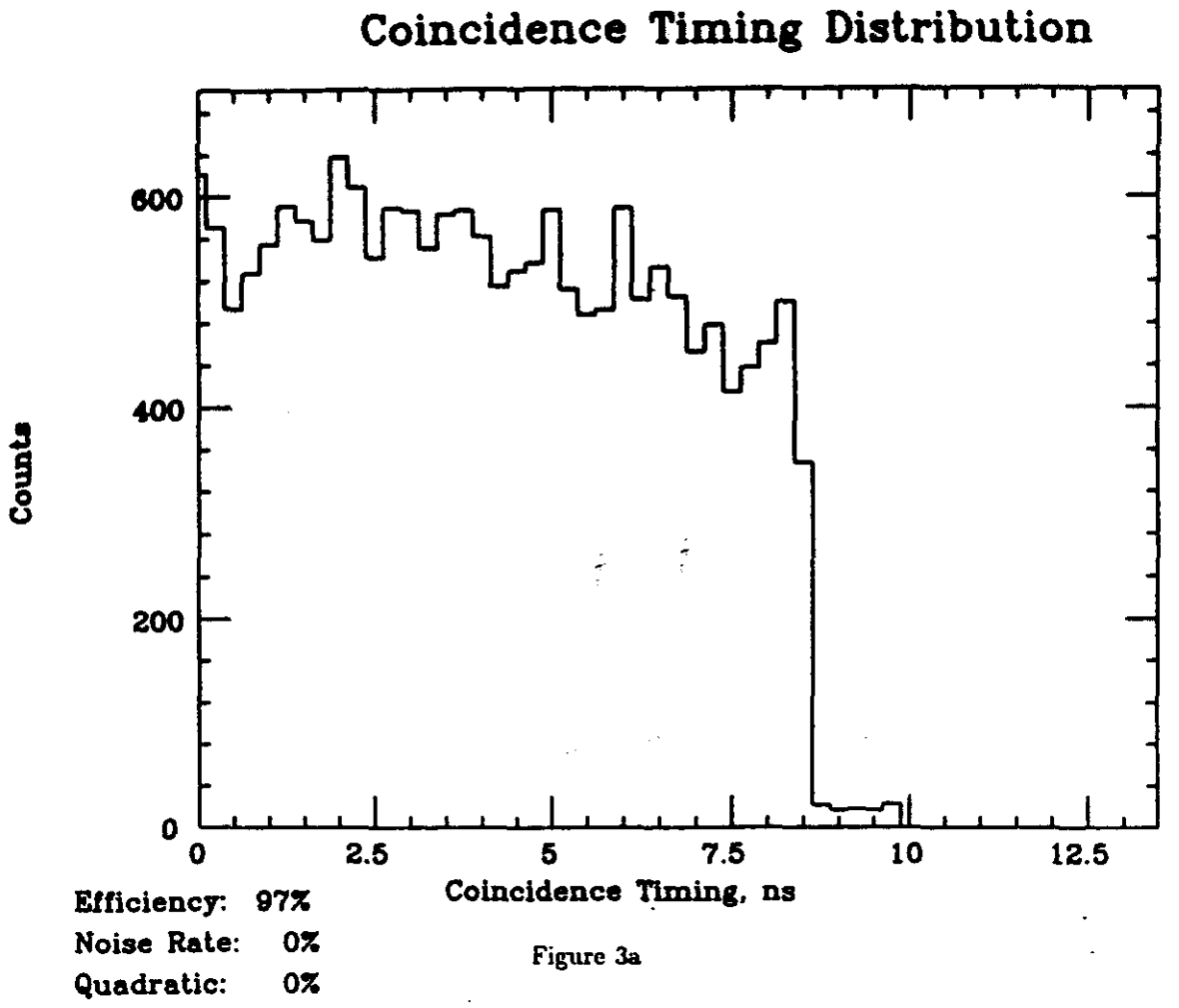

Figure 3a

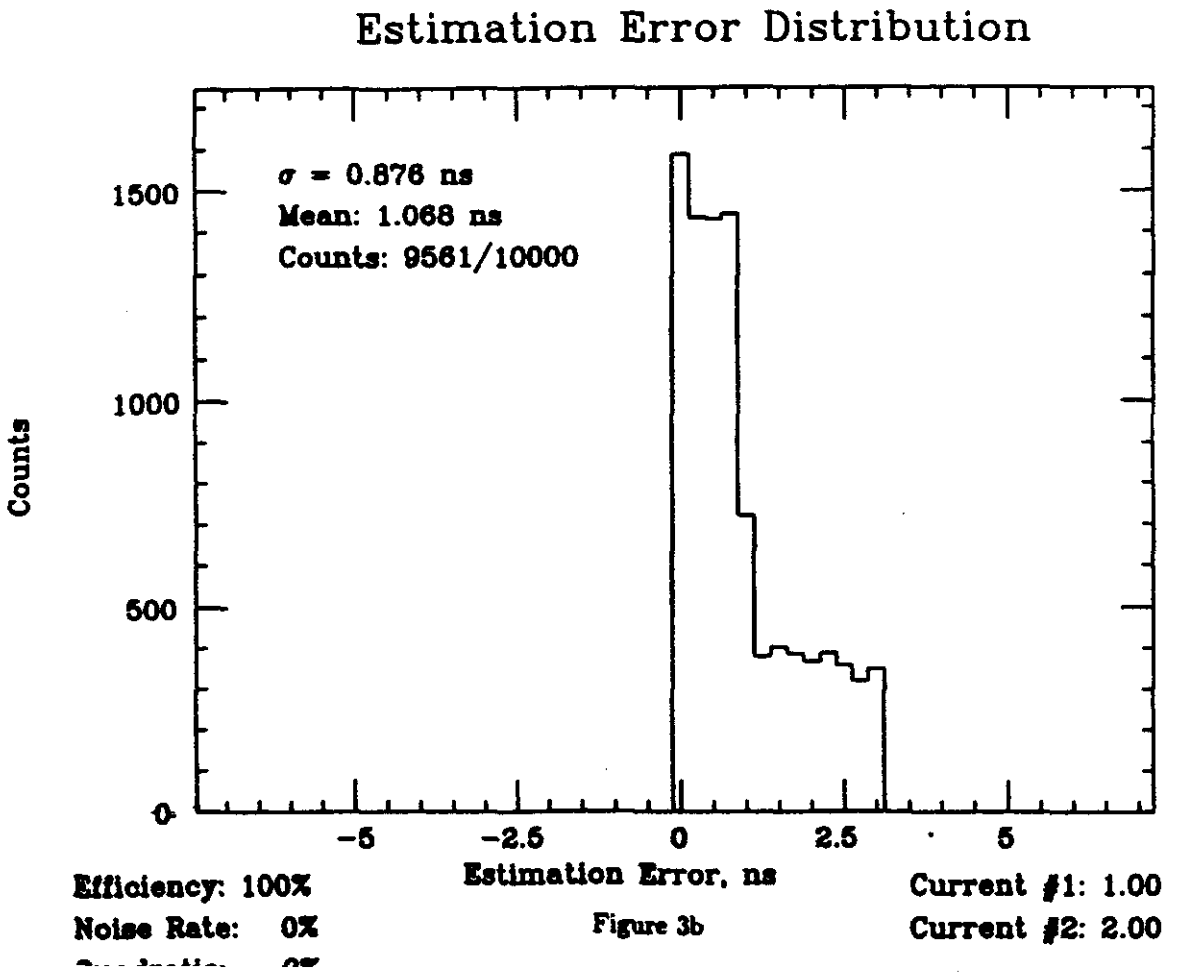

Figure 3b

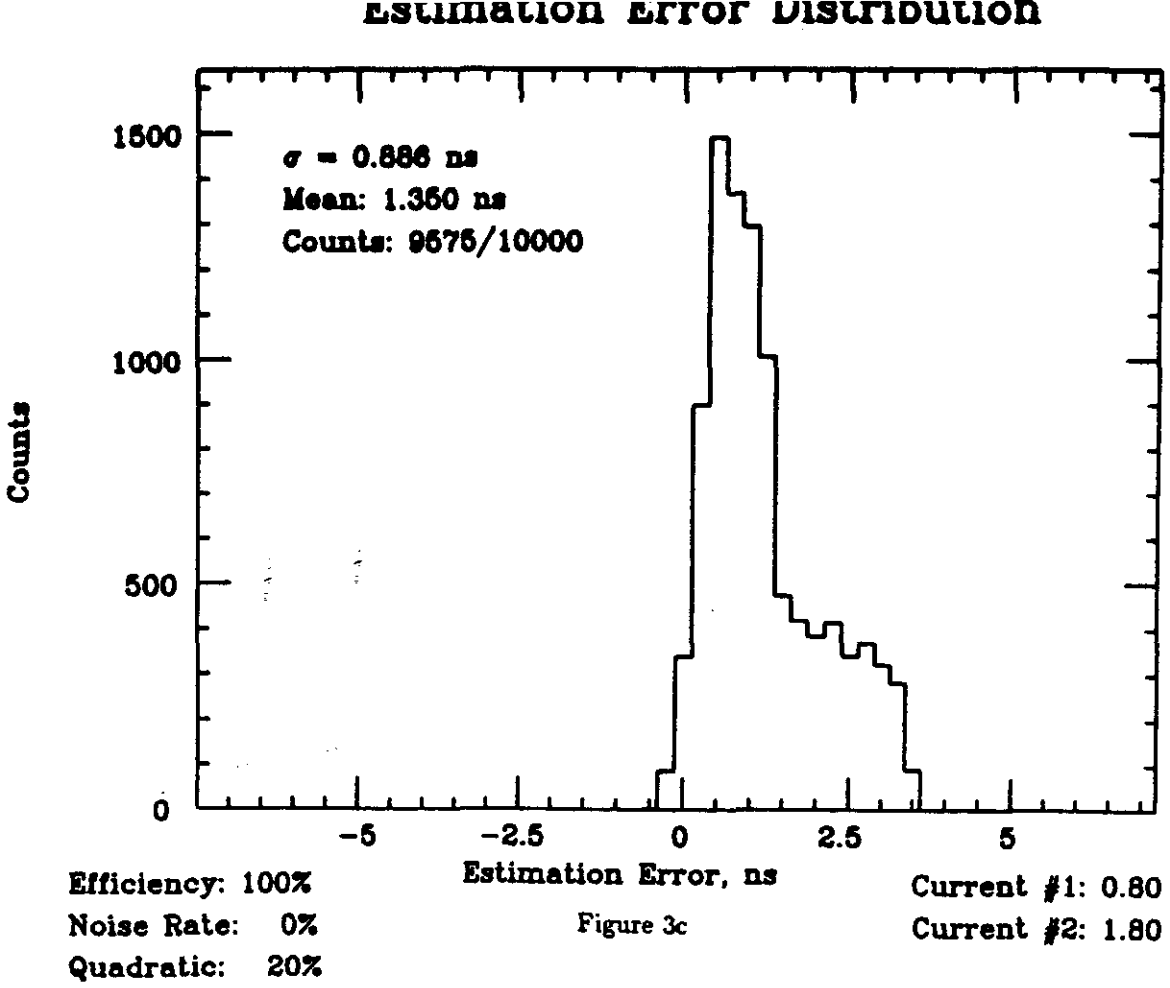

Figure 3c

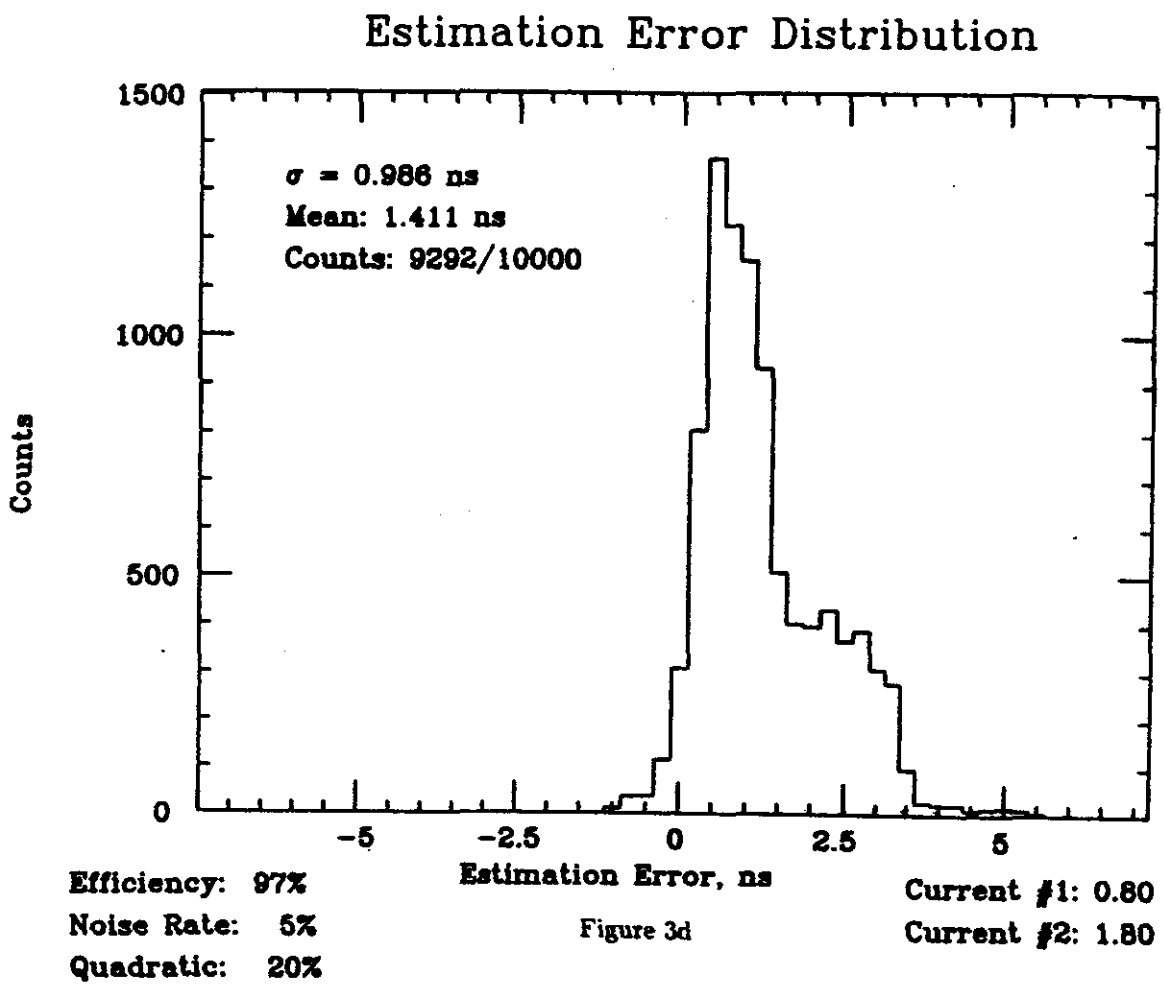

Figure 3d

satisfied with a random hit. Random hits also produce an increased inefficiency when a random hit disables a tube from contributing to the coincidence. Random hit inefficiencies, like individual tube inefficiencies, do not change the optimized current value though the random hits do increase the σ of the timing distribution by about 15%. Table 1 summarizes the effects of tube inefficiencies and random hits for a few choices of parameter values. The currents have been optimized for all cases represented in the table.

Table 1			
Tube Efficiency	Random Hit Rate	Non-linearity	Overall Efficiency
100%	0%	0%	95.6%
97%	0%	0%	93.6%
95%	0%	0%	91.5%
100%	5%	0%	95.0%
100%	10%	0%	94.8%
100%	0%	10%	95.4%
100%	0%	20%	95.8%
100%	0%	40%	95.7%
97%	5%	20%	92.9%

For non-linear parameters away from zero the current optimization has more significance. The minimum σ of the timing distribution was determined for a few values of non-linearity parameter. It is plotted as a function of the non-linearity parameter in Figure 4. From this plot one can see that the timing jitter can be made nearly as small with non-linearities as it is in the linear case if a suitable choice of currents is made. Non-linearities as large a 40% can be tolerated. The plot of Figure 3d shows the timing distribution for a typical set of tube and detector characteristics. The tube efficiency is taken to be 97%, the random hit rate to be 5% in the full drift time, and the drift velocity of the tubes is taken to be 20% less at the full radius than near the wire. The jitter in the arrival time of the pulse is less than ±5ns. The composite efficiency of the system is ≈93%.

The "false" trigger rate of the circuit was studied by the introduction of high level of

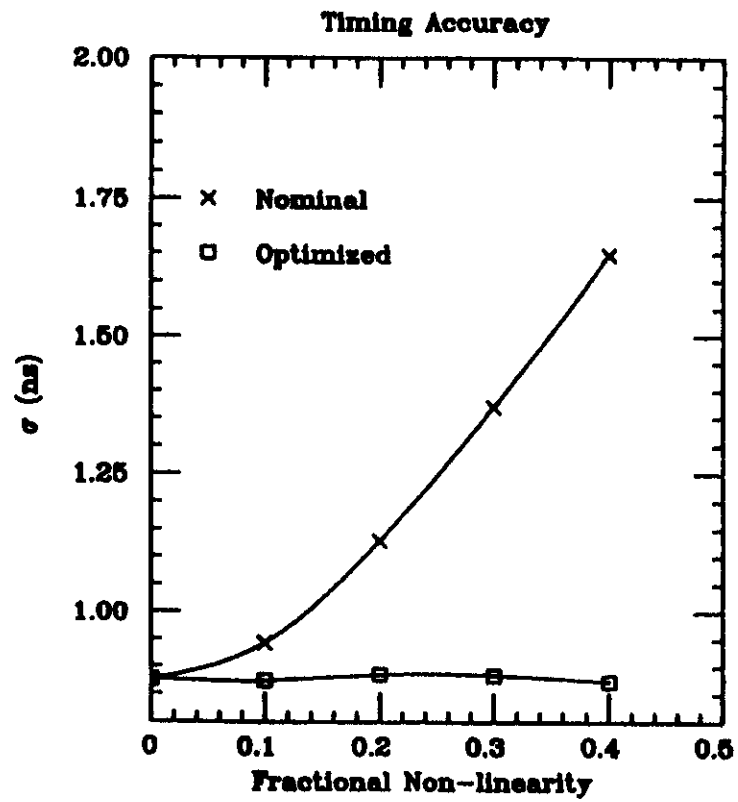

Figure 4

random hits in the absence of any stiff track signal. Figure 5 shows the circuit fractional output rate within a ±5ns window centered on the stiff track time for various random hit rates. Less than 1 in 1000 of the 50ns drift intervals will give a stiff track signal under the extreme conditions where 20% of the tubes have hits in every 50ns interval.

Triad Track Elements

The Circuit

Figure 6 exhibits a circuit that is designed to provide the a fixed delay signal, T_0, for a triad with the center cell staggered 1/2 cell width from the other two. A pattern of this type is shown in Figure 1b. Sufficient information is available in triads to relax the requirement of normal incidence. The three drift times are related by the equation, $t_2 + \frac{t_1+t_3}{2} = r/k$ in the approximation that the times are linear functions of the distance. This equation can be rearranged and written in terms of time differences as

$$\frac{t_1 - t_3}{2} + (t_2 - t_1) + 2 \times (\frac{t_1 + t_3}{2}) = r/k$$

Each term of the equation can be compared to part of the circuit of Figure 6. The first term is generated as a voltage on the capacitor by integration of the current i/2, the second term is added by the integration of the current i, and the last time period is determined by the requirement that the voltage reach the maximum drift time with a current of 2i. The last time period begins at the instant that all drift pulses are received which in this example is t_3. The delay period is precisely that needed to extend t_2 to a full drift period. Although the analysis of the circuit has been represented in the case where the times are ordered $t_3 < t_1 < t_2$, the circuit correctly delays the output T_0 in all combinations of ordering.

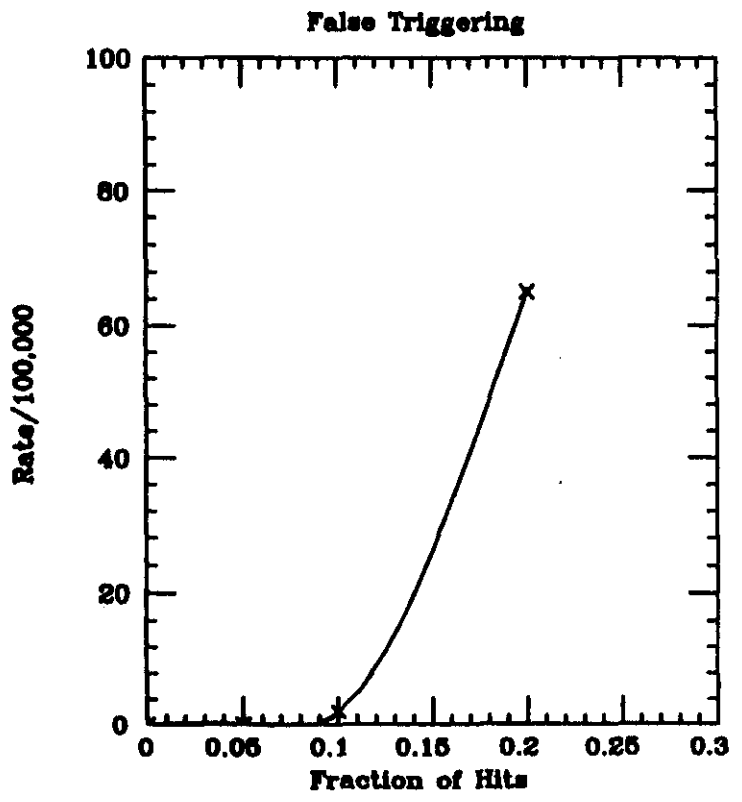

Figure 5

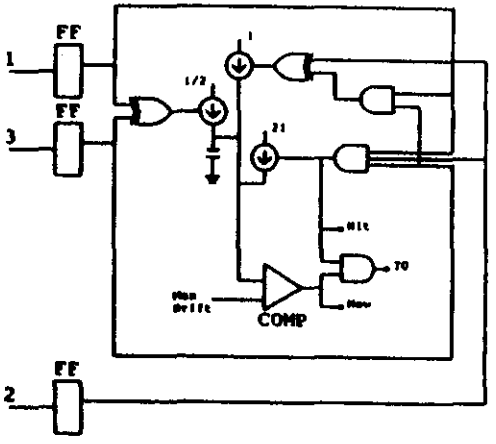

Triad T0 Generator

Figure 6

Calibration

Since there are three currents in the triad synchronizer, there are three conditions where the output, T_0, can be calibrated to zero error. If only the flip-flop associated with wire 1 is set, the current i/2 alone ramps up to the maximum drift time voltage. This generates T_0 at a time equal to twice the maximum drift time. If both wire 1 and 3 flip-flops are set at the same instant, only current i is enabled. Likewise if all three flip-flops are set, only current 2i produces the ramp and hence determines the timing of T_0. These three test patterns can be used with an externally supplied timing interval to separately set the magnitudes of the three currents. Such separate adjustments will permit errors in the generation of T_0 due to non-linearities in time-distance to be minimized.

Simulation

A computer simulation of a triad was undertaken to determine the timing accuracy that can be obtained with a scheme of this type and typical drift tubes. The simulation takes into account the non-linearities in the time-distance relation for rectangular tubes and in the effects of tubes with different aspect ratios. The effectiveness of the auto-calibration

was also evaluated. Each of these simulations was carried out with a uniform distribution of track positions and angles. The angle variation was limited to $\pm 10°$ from the normal to the plane of the tubes.

Results

The three tube circuit has the advantage that the distribution of output times has a zero width when the track passes between the wires at an angle to the normal whose cosine can be approximated by 1, when the distance-time relationship is linear, and when there are no random hits to confuse the electronics. This ideal distribution is shown in Figure 7a. Tracks passing outside of one of the wires produce a distribution of T_0 times as shown in Figure 7b. Some fraction of these *left-right* ambiguity tracks, those near the wire, yield output pulses near enough to the correct T_0 to appear as good track candidates. The remining ones do not and must be considered as contributing to the inefficiency of the scheme. To this inefficiency one must add that due to geometry and that due to individual tube inefficiencies. The overall system efficiency is presented in Table 2 for a few individual tube efficiencies.

Table 2

Aspect Ratio	Tube Efficiency	Random Hit Rate	Non-linearity	Overall Efficiency
1/1	100%	0%	0%	90%
1/1	97%	0%	0%	82%
1/1	95%	0%	0%	77%
1/1	100%	5%	0%	84%
1/1	100%	10%	0%	78%
1/1	100%	0%	10%	90%
1/1	100%	0%	20%	91%
1/1	100%	0%	40%	92%
1/1	97%	5%	20%	77%

A 4cm width tube is assumed for the case where three tubes are used. The drift times associated with these larger tubes is hundreds of nanoseconds. A greater degree of timing accuracy is thus required if one is to identify the track passage time to within 10ns. The

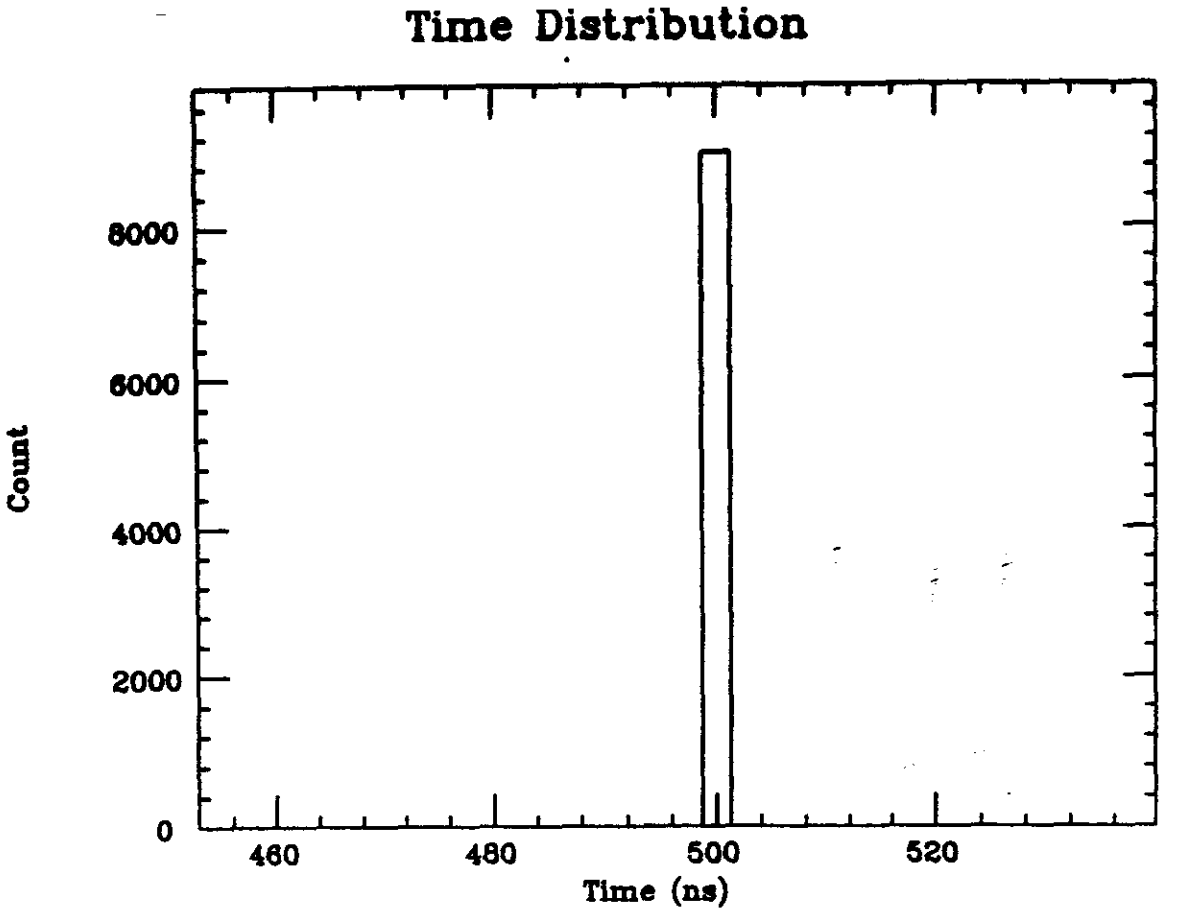

Figure 7a

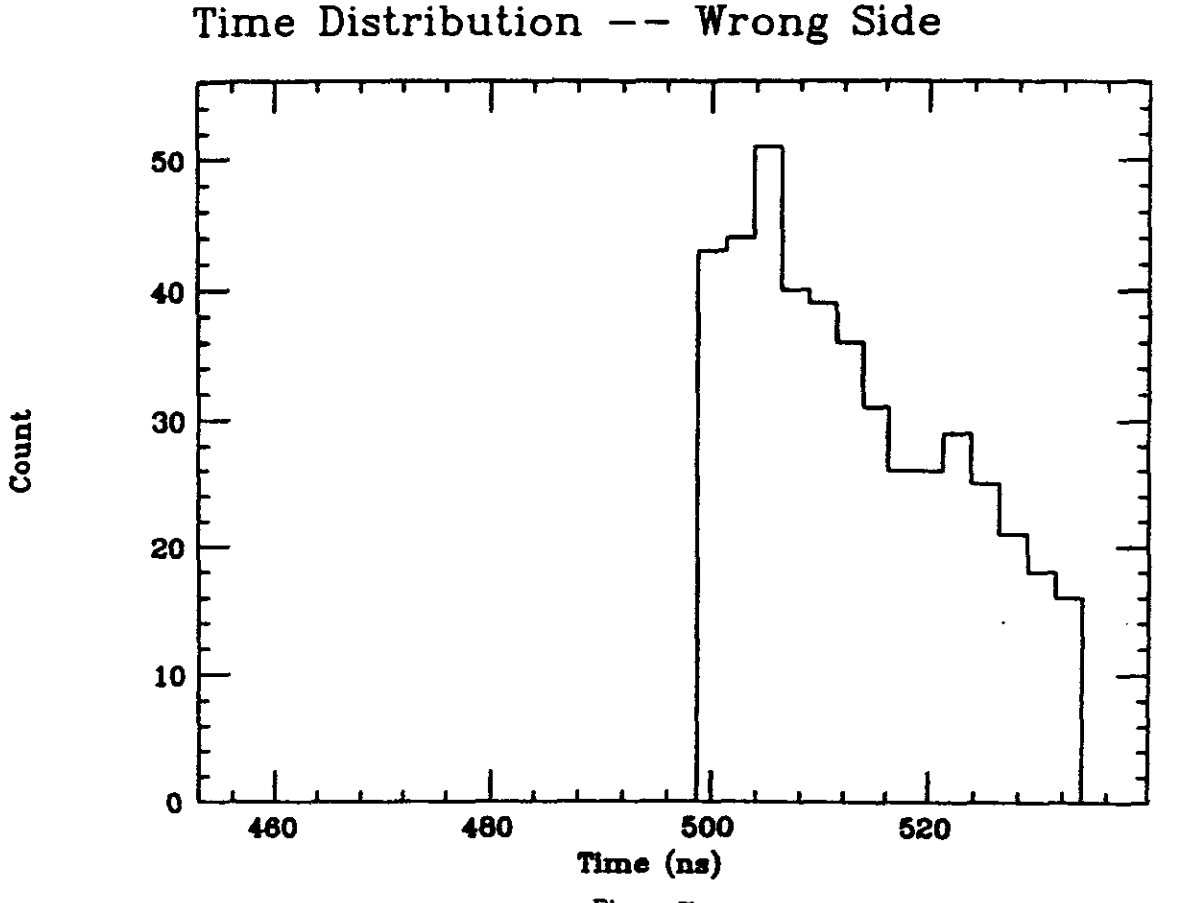

Figure 7b

non-linearities appear capable of distroying the practicality of the circuit given the greater accuracy required. Again the technique of current optimization will be used to minimize the σ of the timing distribution. Figure 8 shows the σ of the timing distribution for non-linear terms ranging from 0 to 40% with the nominal currents and with the optimized currents. Optimization leads to an almost constant σ up to the highest non-linearities studied. It should be noted that the process of current optimization does result in a shift in the peak of the timing distribution. This has the same effect at the addition of a section of cable. Figure 9 shows a timing distribution for 20% non-linearity, 97% tube inefficiency, 5% random hits, and tube aspect ratio of 1/1. The efficiency for sensing tracks is 77% in these assumed conditions. The timing jitter of the output pulse is contained within ±5ns.

Tables 3 and 4 exhibit the characteristics of tubes with other aspect ratios. The largest aspect ratio gives the best efficiencies since the effect of the *left-right* ambiguity is reduced in high ratio tubes. Drift non-linearities and tube efficiencies increase with tube aspect ratio and a practical tradeoff with an aspect ratio of less than 3/1 is likely.

Table 3

Aspect Ratio	Tube Efficiency	Random Hit Rate	Non-linearity	Overall Efficiency
2/1	100%	0%	0%	95%
2/1	97%	0%	0%	87%
2/1	95%	0%	0%	81%
2/1	100%	5%	0%	88%
2/1	100%	10%	0%	82%
2/1	100%	0%	10%	95%
2/1	100%	0%	20%	96%
2/1	100%	0%	40%	96%
2/1	97%	5%	20%	81%

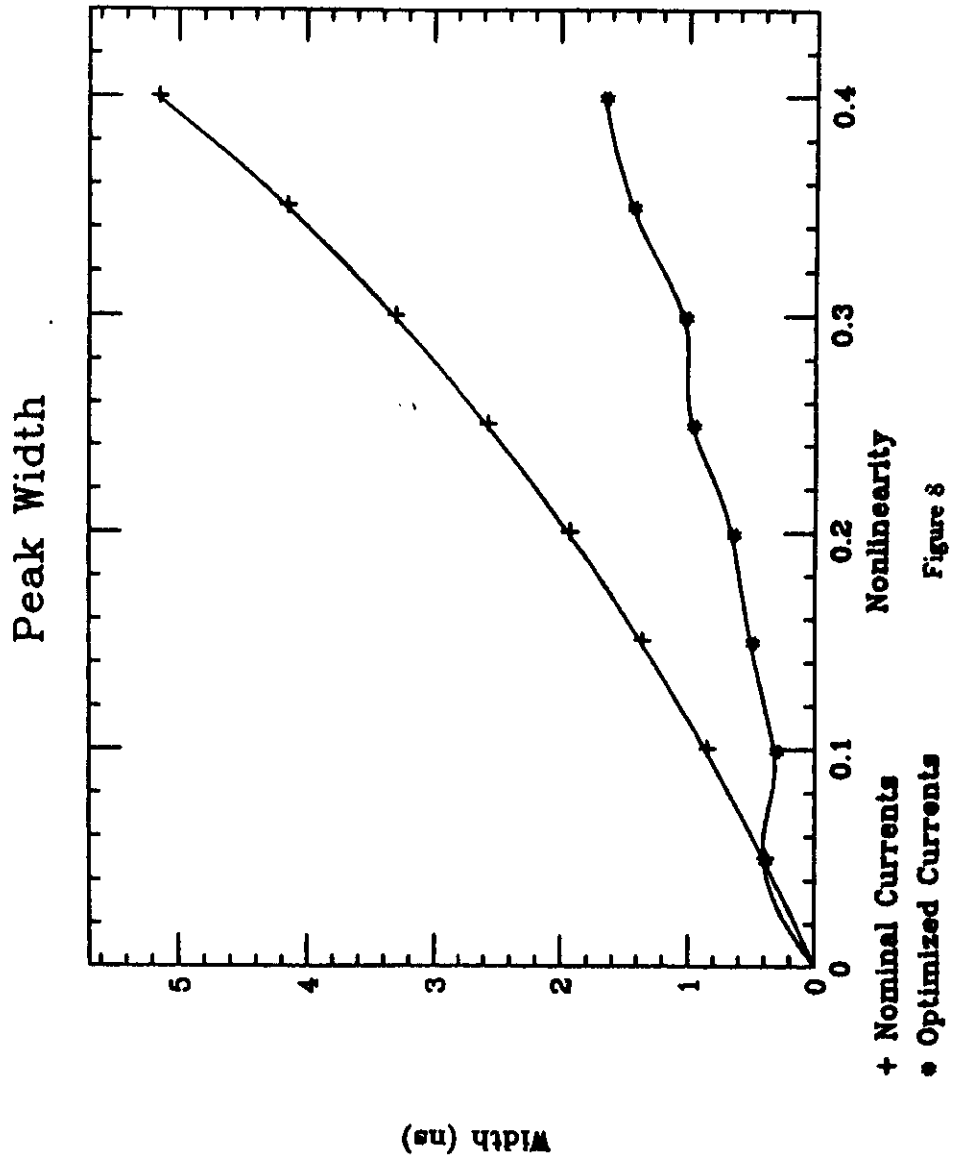

Figure 8

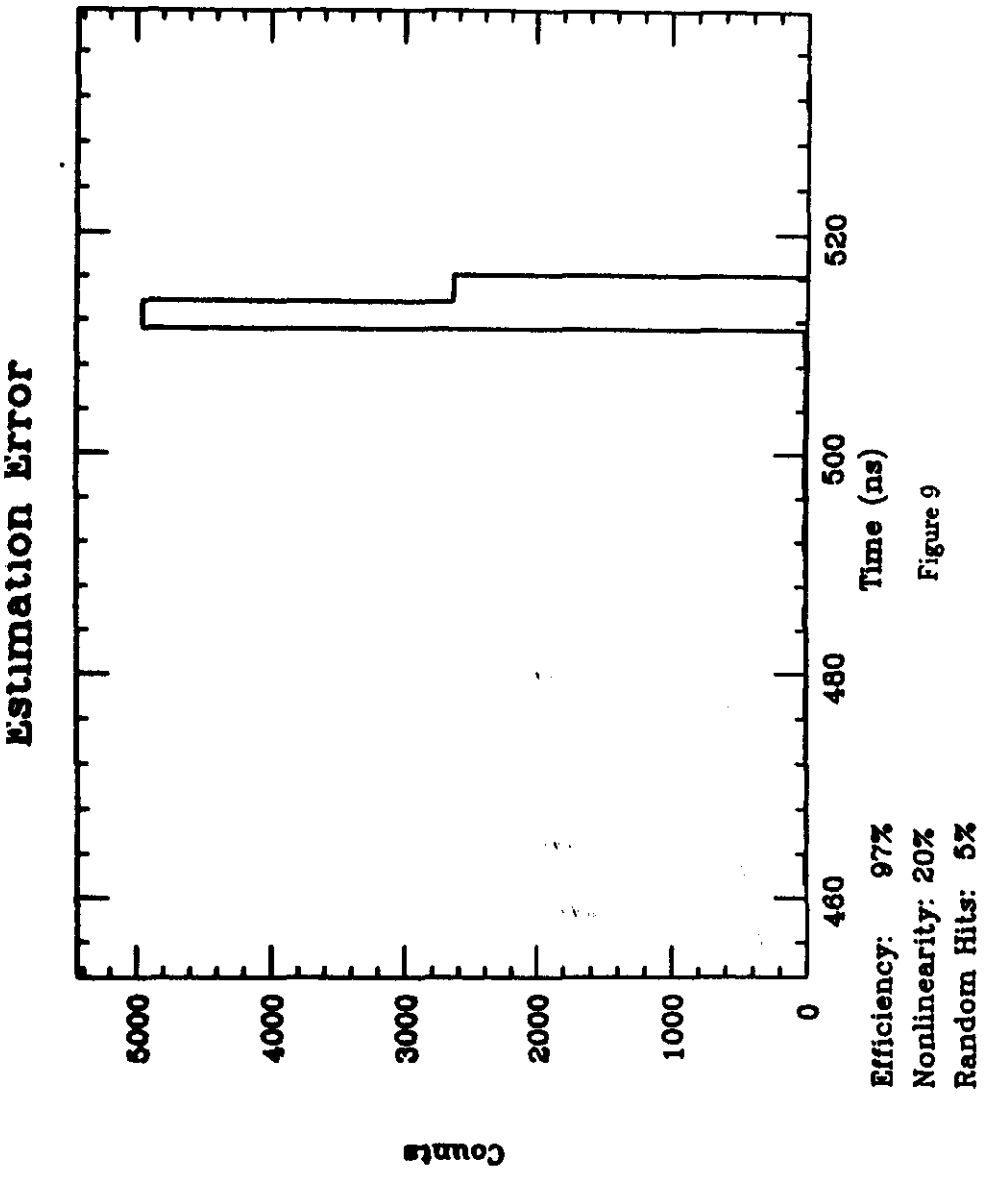

Figure 9

Table 4				
Aspect Ratio	Tube Efficiency	Random Hit Rate	Non-linearity	Overall Efficiency
3/1	100%	0%	0%	97%
3/1	97%	0%	0%	88%
3/1	96%	0%	0%	83%
3/1	100%	5%	0%	90%
3/1	100%	10%	0%	83%
3/1	100%	0%	10%	97%
3/1	100%	0%	20%	97%
3/1	100%	0%	40%	98%
3/1	97%	5%	20%	82%

Conclusions

The proposed approach holds promise as an aid in the solutions for the major SSC problems of associating and collision tagging drift chamber hits. Work is continuing on how to use the information from such circuits for trigger generation and hit tagging. Clearly the same technique can be used to eliminate time variations that result from different track positions in long tubes if signals are extracted from both ends. Use of data from such disjoint locations (on the ns scale) awaits a better understanding of how to optimize the local signal handling, however. An implementation of the triad processing circuit is being developed for evaluation. It was chosen since it will function for evaluation of the straw tube circuit if the inputs 1 and 3 are bridged together and an external coincidence is provided. With regard to long range implementation for SSC detectors, it should be noted that the components used in the circuit are very similar to those studied by Williams[9] for drift chamber timing and pipeline storage. The inclusion of synchronizers within the integrated circuits being developed for those storage and readout functions is a simple extension of the circuits.

REFERENCES

1. G. Hanson *et.al.*, Tracking Simulation and Wire Chamber Requirements for the SSC, Snowmass '88, High Energy Physics in the 1990's
2. R. Thun, Prospects for Wire Chambers at High Luminosity, Snowmass '88. High Energy Physics in the 1990's
3. H. H. Williams *et.al.*,Front End and Signal Processing Electronics for Detectors at High Luminosity Colliders, Submitted to Trans. Nucl. Sci. Vol 36, 1989

APPENDIX C

PROPOSAL TO DEVELOP SSC TRIGGERS BASED ON THE TECHNIQUE OF NEURAL NETWORKS

——UPDATED SEPTEMBER 1989——

Myron Campbell
University of Michigan

Bruce Denby
Fermi National Accelerator Laboratory

ABSTRACT

We propose to investigate the use of Neural Network technology for triggering at the SSC. As a first test of principle, we will build a neural net based B-trigger, operating on calorimeter data, which will identify electrons in jets, and will be tested parasitically in the next run of the CDF experiment in 1991. We will also carry out software simulations to assess the efficacy of neural networks for a suite of generic SSC pattern recognition problems, and consult with neural network researchers both at universities and in industry about optimal algorithms and about how these systems can be cast in hardware. We hope to make sufficient progress in neural tracking and secondary vertex finding to be able to use these to augment the above B-trigger, and test this in the 1993 run of CDF. We request a total of $405,316, for U. of Chicago and Fermilab, which will cover hardware construction, equipment, the hiring of persons to assist with construction and software simulations, and consulting.

PROPOSAL TO DEVELOP SSC TRIGGERS BASED ON THE TECHNIQUE OF NEURAL NETWORKS

I. MOTIVATION

A. SSC Triggering and Pattern Recognition

At the SSC, there is a need for very fast, robust pattern recognition at the trigger level. Since the response times of most existing and forseeable detectors is greater than the 16 ns. bunch crossing time, when a trigger occurs, some of the signals read out from the detectors will indeed have come from the event which caused the trigger, but others will be portions of signals from previous or subsequent events which fall into the readout time window. The only difference between the in-time signals and the out-of-time signals is that the in-time signals will form plausible coherent spatial patterns, such as smoothly curving tracks that point at calorimeter clusters of appropriate energy, and the out-of-time ones will not. Pattern recognition is thus a special problem at the SSC in the sense that we are obliged to perform it even to determine *which* data we should be looking at. The problem is exacerbated by the high probability of multiple interactions per bunch crossing at the SSC (46 percent of crossings have more than one interaction). In these cases it is also necessary to determine which data are associated with the interaction that produced the trigger.

Most triggering schemes for the SSC propose a 3-level system. In level-1, prompt cuts, such as total E_T, missing E_T, number of clusters, presence of muon, etc., will be used to produce a reduction of perhaps a factor of 1000. This leaves the additional factor of 10^4, needed to get the rate to tape to an acceptable level, up to levels-2 and 3, which will have to use non-prompt cuts, including 'physics' cuts. This implies that levels-2 and 3 at the SSC will rely very heavily on pattern recognition, since identification of particular topologies is usually what one means by 'physics' cuts. Such a rejection factor has never been obtained to date in a High Energy Physics experiment (CDF achieves a *total* reduction of about $5 \cdot 10^4$). Also, one would like to be able to create sophisticated triggers based on complex patterns, such as, for instance, $Higgs \rightarrow W^+W^- \rightarrow 4jets$.

Heavy quark spectroscopy is one domain in which the requirements placed on pattern recognition are even more severe. The SSC running at a luminosity of 10^{32} and with a reconstruction efficiency for b-quark events of 1 percent is roughly equivalent to a 100 percent efficient e^+e^- B factory running at a luminosity of 10^{36}. B events will be 'soft', with a mean p_T of 6 Gev/c, and will produce decay leptons of only 1 to 2 Gev/c. In order to separate B events from the background, it will be necesary to use tracking and secondary vertex finding, at the trigger level.

There is also a problem at the offline level. The Fermilab ACP system addressed the offline reconstruction problem by exploiting event parallelism on arrays of processor nodes. Recently, experiments have increased the data produced and code complexity by orders of magnitude (e.g., E769, E791, CDF), to the point that offline reconstruction is again a bottleneck. Needless to say, the situation will be worse at the SSC. Pattern recognition, especially tracking, is normally the biggest, slowest piece of code in a High Energy Physics experiment. Fast pattern recognition would also enormously aid the offline situation.

B. Neural Networks

In the past few years, one has heard a great deal about the pattern recognition capabilities of a new technology called Neural Networks, a form of fine grained massively parallel

processing. These are highly interconnected arrays of simple nodes which communicate with each other via analog levels. The behaviour of a single node is described by

$$O_i = \Theta[\sum_{j=1}^{n} T_{ij} O_j - V_{th}]$$

where O_i is the output of node i, T_{ij} is the connection strength from the output of node i to the input of node j, V_{th} is a threshhold voltage, and Θ is a function of 'sigmoid' shape. In the high gain limit, the sigmoid function approaches a step function, which can be interpreted as representing a '0' or a '1'. In this way the neurons can represent binary information. Neural Networks, implemented in silicon, have been shown to solve certain pattern recognition problems (e.g., handwritten character recognition) on a time scale of hundreds of nanoseconds [1], and may thus be an appropriate technology for application to High Energy Physics triggering and data analysis.

These networks have been studied since the 1940's, but since about 1982 the field has experienced a resurgence that can only be called explosive. There are currently thousands of researchers active in the field, and almost every university has someone working on neural networks. The International Neural Network Society has just been formed, and there are several professional journals dedicated to neural nets. The California Institute of Technology recently created a new department called Computing and Neural Systems. Research in neural networks is going on in robotics, machine vision, identification of sonar targets, classification of radar returns, speech synthesis, data retrieval systems, and a long list of other fields.

C. Proposal

Most applications involve some kind of pattern recognition, or combinatorial optimization. Both of these are common to problems in High Energy Physics data analysis. We propose to form a neural network study group consisting of ourselves, a post doc, and a student, and in consultation with researchers in the field, to demonstrate ways in which neural networks may be of use in addressing the special pattern recognition problems that will be encountered at the SSC.

The thrust of the proposal is to investigate the application of neural network technology to a suite of generic High Energy Physics problems, while keeping closely attuned to currently running experiments to identify possible proving grounds in those experiments for techniques developed in the course of our studies. In the case of a B trigger, first using a 'feed forward' calorimetry based device, and later, secondary vertex finding, a proving ground already seems possible within the context of the CDF upgrade at Fermilab, as we shall discuss below.

IV. DESCRIPTION OF TECHNIQUE

A. Feed Forward Networks

It has been shown by Rosenblatt in 1958 that a single layer neural network can be trained in a finite number of steps to separate patterns. The set of patterns must be linearly separable, i.e. there must exist a hyperplane in the space of all input variables which separates input patterns into two classes. This hyperplane does not have to be found in order for the network to classify the patterns, it only has to exist. A suitable set of training vectors whose classification is known must also be available.

This can be translated to the application of recognizing patterns in a trigger for an SSC detector. One can take the set of signals measured from the detector to form an N dimensional space, e.g. a 10,000 dimension space made from the responses of all calorimetry cells. If the

events of interest (signal) lie on one side of a hyperplane in this N dimensional space then a single layer neural network can be trained to separate signal from background. The simplest example of a hyperplane would be to hold one of the input variables constant. The easiest way to differentiate signal from background in this case would be to use a discriminator on the value of the single variable. Many classes of patterns have simple criteria such as a threshold on a single variable or simple function of a few variables, and these classes of problems are best solved by conventional techniques. The power of the neural net algorithm comes into play when the description of the classifying hyperplane becomes very complicated. That signatures for specific physics processes in the SSC environment are difficult to separate from background indicate that the techniques of neural networks will have application.

The ability to train multiple layers of feed forward nets have extended the range of problems which can be solved. The most famous example is the exclusive-or problem. Since this is not linearly separable it can not be solved with a single layer. However three neurons connected in two layers can be trained in about 25 steps to separate the exclusive- or. Application of this technique to electron/jet discrimination has been done by Cutts et al. [6], showing that a neural net based solution can obtain better efficiency and rejection than conventional algorithms.

B. Feed-back Networks

For simple pattern classification tasks with a one to one correspondence between input data and output responses, feed forward networks are indicated. For some problems, though, the patterns cannot be simply characterized, but, rather, consist of related subelements which may occur in an essentially infinite variety of configurations. A vertex, for instance, will always consist of a set of tracks emanating from a point, but the relative angles between tracks can take on an infinite number of possible values, making characterization difficult. The task of the neural network for this type of problem is to segment the image into groups of mutually reinforcing elements. These associations into groups can only be accomplished by allowing each element to test the viability of its membership in each group and finally decide upon one. This implies an iterative nature to the calculation, and recurrent, or feedback networks are thus required.

Recurrent networks have been popularized by Hopfield [7]. Connections between neurons are are symmetric, $T_{ij} = T_{ji}$, and $T_{ii} = 0$. The behaviour of the network is characterized by the equations [7],

$$\tau \frac{dv_i}{dt} = \sum_{j=1}^{N} T_{ij}\Theta(v_j) - v_i$$

where Θ is a sigmoid output function, v_i is the input value of neuron i, T_{ij} is the coupling strength or coefficient between neurons i and j, and τ is the integration time constant of the network. It can be shown [7] that for such a network, there exists a Lyapunov function

$$E = -\frac{1}{2}\sum_{i,j=1}^{n} T_{ij}\Theta_i\Theta_j$$

which is continuously minimized as the network evolves. The network starts at an arbitrary configuration, evolves to a fixed point of the system (local minimum of the energy) and stops there.

The application of this technique consists of

1) Defining the neuron. What shall the neuron represent in a given application?

2) Defining the connection neighborhood. Which neurons are connected to which others?

3) Defining the T_{ij}. What form of the connection strengths is appropriate for the problem at hand?

These three properties should be defined in such a way that the fixed points of the system correspond to the desired 'answers'. Let us consider the example of track finding as outlined in [3]. The neuron is defined as a link between two points which could possibly be on the same track. The connection neighborhood can be of the order of a few times the mean separation between points on a track (distance between wire planes, e.g.). The connections strengths were chosen to have a form

$$T_{ij} = \frac{A \cdot cos^n \theta_{ij}}{r_i r_j}$$

where θ_{ij} is the angle between the links i and j, and r_i and r_j are the lengths of the links. This ensures that we will join together links which are locally nearly collinear. The result of the network evolution is to produce sets of mutually reinforcing links which chain together to form the tracks. Some simulated results of applying this method to track finding in a TPC with magnetic field are shown in figure 1 (from reference [4]).

V. PROPOSED ACTIVITIES

A. Calorimetry Based B Trigger

We propose to construct a trigger using feed forward neural networks. The goal of the trigger is to separate the decay $b \rightarrow e\nu c$ from jet background. The inputs to the trigger will be the response from the segmented electromagnetic and hadronic calorimeters of CDF [8]. This project was chosen for several reasons:

1) Although there are many differences, the CDF detector is currently the most similar running detector to an SSC detector in terms of luminosity, event characteristics, and calorimeter segmentation.

2) The experience gained from solving problems encountered in building a device which must operate in a real environment will be valuable in building an SSC trigger.

3) The ability of being able to trigger on a new class of events is appealing enough to the CDF collaboration that the disruption caused by the installation of this device will be tolerated.

4) The particular problem of separating electron decays of b quarks with hadronic overlap probably can not be solved by conventional techniques such as are in place at CDF.

5) There exist detailed Monte Carlo generation and accurate detector simulation which are needed to provide the training vectors.

6) Due to the speculative nature of this project, funding through other High Energy Physics Grants would not be possible.

The device will be implemented in a set of two Fastbus crates in the trigger room at CDF. The analog signals from the calorimeter are corrected for gains and biases by the existing RAW cards [2] and transmitted to the existing CAS cards via a front panel jumper (see fig. 2). These signals will be tapped from this jumper by unity gain amplifiers and sent to the new Analog Receive/Shifter. There are 2016 signals forming a 24X42 array of hadronic and electromagnetic information. The dimensionality of the problem will be reduced from 2016 to about 64 by selecting a region of interest. The existing cluster finder will send the coordinate of each cluster to the new shifter control. This will then direct the analog receiver/shifter to transmit the relevant analog signals to a backplane. The backplane will be built on the auxiliary segment of the Fastbus crate. The neural net itself will be implemented with a 64 neuron ETANN available from Intel through a non-disclosure agreement.

Any real test of the Neural Net technique will have to have inputs generated and the results read out. As can be seen from figure 2, this project will be taking advantage of a large system which is already in place. The signals from the calorimeter are already shaped and corrected for gains and offsets, the information from the cluster finder is readily available, and the system used to read the results of the neural net is already in place. That large implementations in hardware of the feed forward technique have not been done in the past has been mainly due to the lack of a problem amenable to this technique which needed to be solved in real time [9].

The determination of the interconnection weights will be done in a computer simulation of the trigger. Several commercial packages are available for assistance in training feed forward networks, but we have written our own software in Fortran during the summer of 1989. The set of training vectors will be provided by Monte Carlo generation of $b\bar{b}$ events (ISAJET), detector simulation, and finally trigger simulation. The result will be a set of 2016 dimension vectors, the coordinates of clusters as found by the cluster finder, and possibly stiff track information. This software already exists within the CDF collaboration.

B. Tracking and Particle Identification

This section of the proposal involves software simulations and consulting with industry and universities concerning possible implementations in hardware. The funds sought here are to cover hiring of additional manpower (one postdoc) to help with simulations, and consulting fees. Because the problems studied are generic and are not tied directly to any existing experiments, these funds cannot be obtained from other sources.

1.) Recurrent Net Approaches

a) Tracking. We plan to study the track finding problem with a view to improving the algorithms. The existing algorithm does not always remove all incorrect links, and, in addition, the question of 'readout', i.e., of how to collate the link information into track quantities for use in triggering decisions has not been adequately addressed. We have established contacts with Prof. Carsten Peterson of Lund, Sweden, a physicist interested in the neural tracking problem and with whom we will be collaborating to try to find optimal algorithms. We have also recently learned of the existence of learning algorithms for recurrent networks and will try this approach as well.

We also intend to continue to explore the use of a neural network for electron identification as outlined in [5]. Here, the centroid of a calorimetric energy deposit is treated as a 'generic' hit, to which links are made just as in the tracking chamber. The survival of a link to a generic hit in an electromagnetic calorimeter indicates good alignment of the hit with the track, which characterizes an electron candidate.

b) Secondary Vertex Finding SEE ALSO MAIN PROPOSAL The problem of primary and secondary vertex finding can be handled in the framework of a recurrent neural network [10]. It is interesting to note that the vertex finding problem can be regarded as a tracking problem by first performing a Hough transform [11] on the tracks [12] (figure 3). Progress in the tracking algorithms will thus be immediately applicable to vertex finding as well.

The first method to be tried will be to treat each crossing of two tracks as a potential vertex, identifying a neuron with each potential vertex, and letting the network evolve until the only vertices remaining are those which correspond to true vertices actually present in the data. This method can be used in conjunction with the associative memory track finding method developed at Pisa [13] for track finding in silicon microstrip detectors. The present algorithm, used after application of the associative memories, uses traditional processors to

group together track crossings which are close together, then counts the number of 'good' crossings and makes a cut on this quantity to enhance the beauty sample. The neural network method sets a bit for each crossing; at the end of the evolution, the number of 'on' bits could be counted to allow the same enhancement cut to be made. Thus the neural network vertex finding method interfaces nicely to the associative memory tracking method. This method suffers somewhat from the 'readout' problem mentioned above for tracking, and we will also be considering ways in which the good crossings can be collated into good vertices within a neural network framework.

We intend to explore actively the possibility of using the associative memory/neural network method as a secondary vertex trigger to be used in conjunction with the beauty trigger mentioned earlier.

c) Stereo Matching The use of tracking layers oriented at small angles with respect to the primary wire direction, or stereo layers, is a common technique to give position information in the dimension not measured by the primary wires. Unfortunately, linking the stereo views with the primary view, in a high multiplicity environment, is a very computationally intensive task. At CDF, for example, this takes several seconds per event on an ACP node.

When the small angle stero layers are at fixed radii, for a given track found in the $r-\phi$ view, the corresponding stereo segments lie on a straight line in $r-z$ space. Typically there will be several 'incorrect' stereo segments from other tracks also present in the $r-z$ plot. The stereo matching thus is reduced to line finding in the presence of noise, and neural tracking techniques can again be used. We will set up a tracking algorithm for a typical small angle stereo configuration and optimise its performance.

d) Cherenkov Photon Assignment In a Ring Imaging Cherenkov counter, RICH, the data consists of a set of charged track hits, and photon hits which lie on rings whose centers are the track hits. In order to perform particle identification, it is necessary to associate the photons with the tracks which produced them. This task can be performed by a neural network. The neuron here is a link between a photon hit and a track hit. Links sharing a photon inhibit each other (since we want a unique assignment), and links which share a track reinforce if their radii are almost the same (i.e., if they are likely to have come from the same track). The network evolves to a configuration in which only the correct assignments remain. We will study this and other choices of neuron, and experiment with various forms for the connection matrix, in order to optimize the performance of the network.

2) Feed Forward Approach

Track Segment Finding in Straw Chambers (SEE ALSO MAIN PROPOSAL)

Associative memory, or pattern matching techniques have been used for some time as an approach to fast track finding. In the software approach, as used, e.g., in E711 at Fermilab and Mark II at SLAC [14,15], one defines a 'track dictionary' which is a list of bit patterns containing one pattern for each possible track. The patterns are defined by indexing all the possible hit positions in the detector, and, for each track, indicating with a '1' those bits which correspond to hits one would expect to be present for the track in question. Track finding is accomplished by masking the actual pattern of hits in an event with each of the stored patterns in turn to see if that pattern is present in the event.

This method has also been implemented in parallel hardware in the form of associative memories, as mentioned above [13].

A limitation of these approaches is that the number of possible patterns becomes very large for large, high resolution tracking systems.

It is interesting to note that the associative memory approach bears some similarities to feature extraction in animal visual systems. In particular, a stored pattern of hits for a small, straight segment, is analogous to the orientation sensitive cells found in animal visual cortex [16]. These cells give maximum response when their visual fields are illuminated by a short, bright bar at a particular orientation.

Pattern matching techniques cover the full angular range by storing a pattern for each possible angle. In the animal cortex, units exist only for a small number of possible angles, perhaps 10 to 20 (the exact number is not known). This indicates a very coarse resolution for determination of angles, several degrees, while it is clear that animal visual systems nonetheless manage somehow to remain sensitive to changes in angle which are much smaller than this. Apparently intermediate angles are encoded as linear combinations of the responses of the existing angular units.

The angular dependence of the match of a stored pattern with a track is essentially a delta function, i.e., the response is essentially zero unless the track lines up perfectly with the mask. The case of the orientation sensitive cells is markedly different: the response of the cell versus angle of stimulus is approximately gaussian with a spread of about 10 degrees. This is because the orientation sensitive units are constructed from subunits whose responses decrease with the distance of the stimulus from the center of the receptive field (called on-center units).

Animal visual systems, then, seem to have avoided the need to encode explicitly all possible line segments by using coarse grained sensitive units to build angle units with coarse resolution, and by encoding angles intermediate to those explicitly defined as linear combinations of responses of the defined units.

This economy in the number of sensitive units could be attractive for triggering systems for High Energy Physics experiments. Multi-layer straw chambers have been proposed as tracking devices for the SSC. If the signal wire of a straw tube is put through a time to voltage converter, the result is a device whose resonse varies linearly with distance of the track from the wire. We will simulate a layered feed-forward network which uses straw tubes in a way analagous to on-center units to build orientation sensitive units, and devise a suitable readout to interpolate between the fixed angles to be able to resolve tracks with good angular resolution (figure 4). A sample of straight track segments will be used to train the network. The effects of the choice of base angles, noise, track overlap, etc., will be studied. Constructing orientation sensitive units from on-center units in a neural net simulation has been accomplished by a group at University of Pennsylvania [16] and we expect to consult with this group during our studies.

3) Hardware and Algorithm Research

The feed forward network for the calorimetric application mentioned earlier appears to be the simplest of the networks we propose, and thus will be the first to have a true analog hardware implementation. The experience gained here can then be applied to the problems of tracking and vertexing which require substantially higher neuron and connection counts.

In addition, we will make an in-depth market survey of available and soon-to-be available neural network hardware. The field of hardware neural networks is new and it will take some digging to see what exists. Our suspicion at the present time is that no suitable hardware is currently commercially available, but this remains to be verified. We will investigate the building of special purpose VLSI hardware to carry out the desired tasks.

In the course of these investigations we will also be looking for algorithms adaptable to our applications which may have been developed by others. There are today a number of

neural network companies in existence who have developed algorithms for the military, for instance.

This aspect of our work will involve consultation with experts in the fields of electrical engineering and neural networks at universities and in industry.

References

1) *CMOS VLSI Neural Network Models*, H.P. Graf, L.D. Jackel, and R.E. Howard, AT&T Bell Laboratories, Room 4G320, Holmdel, NJ 07733; in *Hardware Implementation of Neuron Nets and Synapses*, workshop sponsored by NSF and ONR, January 14 and 15, 1988, San Diego, CA.

2) D. Amidei et al., *Nucl. Inst. Meth* **A269** (1988) 51-62.

3) B. Denby, *Computer Physics Communications* **49** (1988) 429-448.

4) B. Denby, *Neural Network and Cellular Automata Algorithms*, FSU-SCRI-88-141, Supercomputer Computations Research Institute, Florida State University, Tallahassee, FL 32306-4052.

5) Bruce Denby and Stephan L. Linn, *High Energy Particle Identification Using a Neural Network Algorithm*, in preparation.

6) D. Cutts et al., *The Use of Neural Networks in the D0 Data Acquisition System*, presented at the Conference on Real-Time Computer Applications in Nuclear, Particle, Plasma Physics, Williamsburg, VA, May 15-19, 1989.

7) J.J Hopfield and D.W.Tank, *Biological Cybernetics* **52** (1985) 141.

8) The Collider Detector at Fermilab. Reprinted from *Nucl. Inst. Meth* A, North Holland, 1988.

9) John Hopfield, private communication.

10) B. Denby and S.R. Amendolia, work in progress.

11) P.C.V. Hough, *Methods and Means for Recognizing Complex Patterns*, U.S. Patent 3,069,654, December 18, 1962.

12) A. Menzione, *Heavy Flavour Tagging in CDF*, INFN PI/AE 85/3, University of Pisa, Department of Physics, Pisa, Italy.

13) M. Dell'Orso and L. Ristori, *VLSI Structures for Track Finding*, proceedings of the International Conference on the Impact of Digital Microelectronics and Microprocessors on Particle Physics, Trieste, 28-30 March 1988, published by World Scientific Pub. Co. ISBN 9971-50-742-0.

14) C. Georgiopoulos et al., *A Vectorized Track Finding and Fitting Algorithm in Experimental HEP Using a Cyber 205*, FSU-SCRI-87-08, Florida State University, Tallahassee, FL.

15) J.J. Becker et al., *Nucl. Inst. Meth.* **A235** (1985) 502.

16) D.H. Hubel and T.N. Wiesel, *Proc. Roy. Soc. London* **B198** (1977) 1.

17) Paul Mueller et al., *Neural Computation of Visual Images*, University of Pennsylvania, Department of Biochemistry and Biophysics, unpublished.

Figure 2. Track reconstruction by recurrent neural network. From Reference [4].

Figure 3.

Figure 4. Constructing orientation selective cells from on-center cells, and comparison with associative memory track finding. From reference [17].

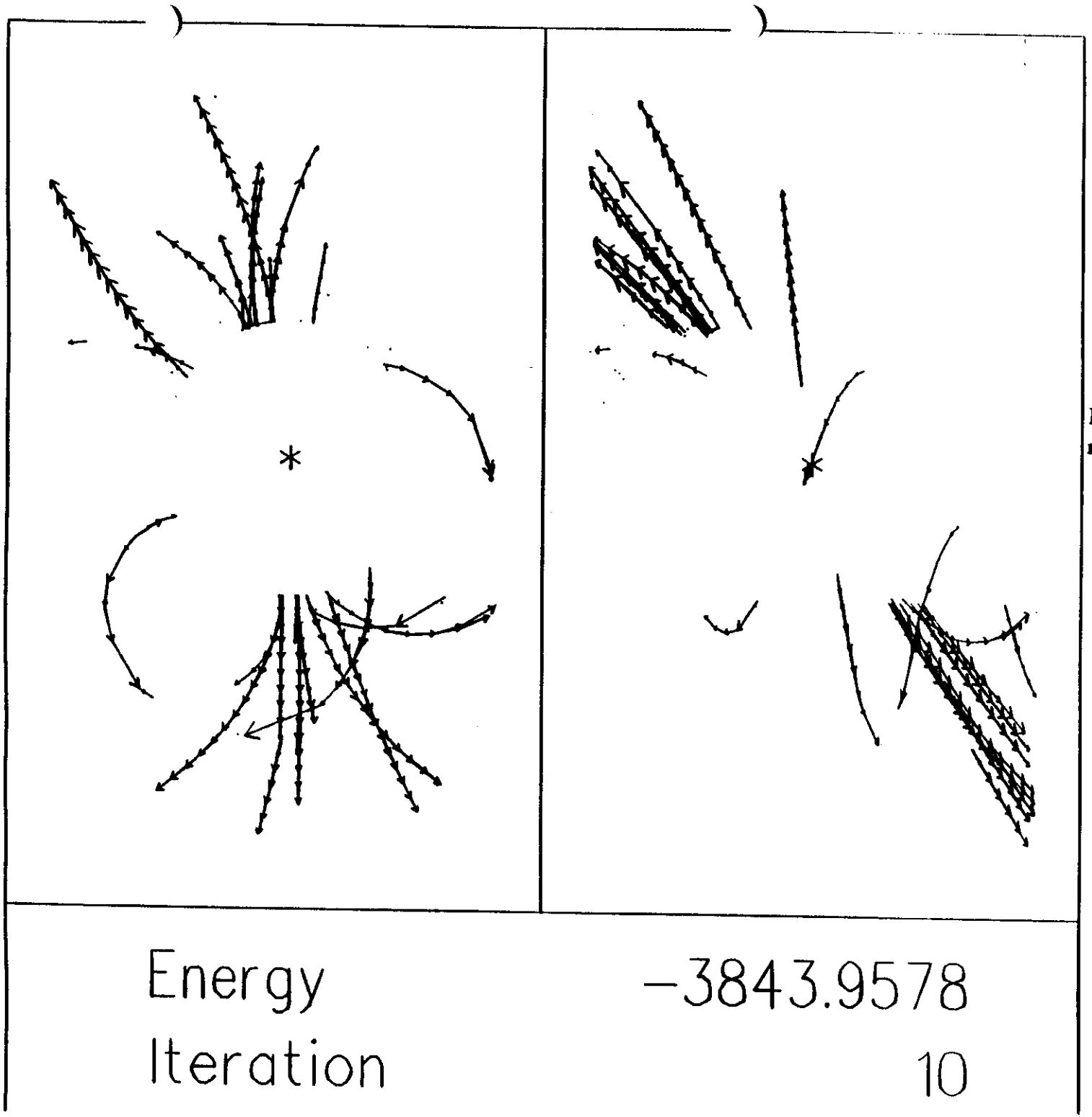

Figure 1. Track reconstruction by recurrent neural network. From Reference [4].

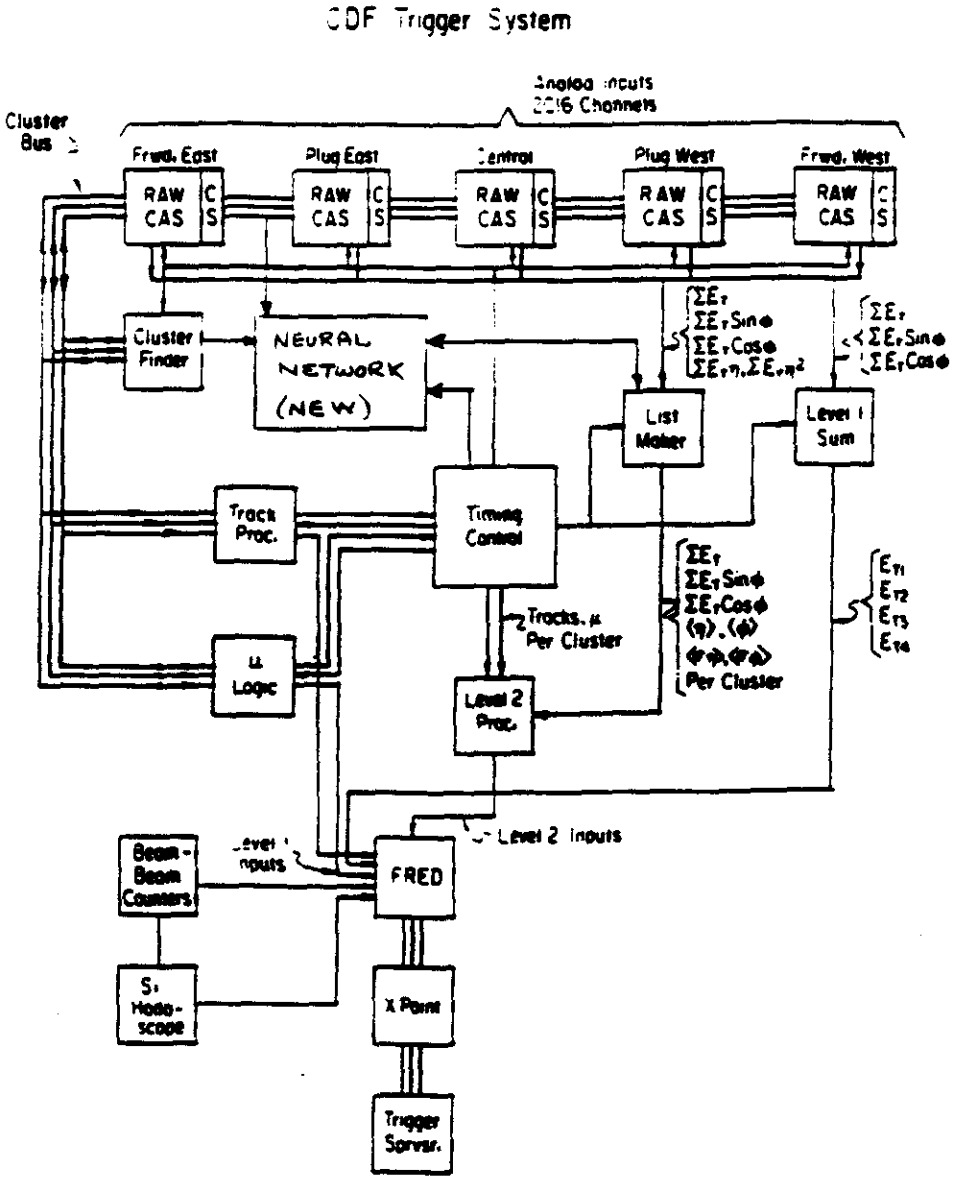

Fig. 2. A block diagram of the CDF Level 1 and Level 2 trigger system.

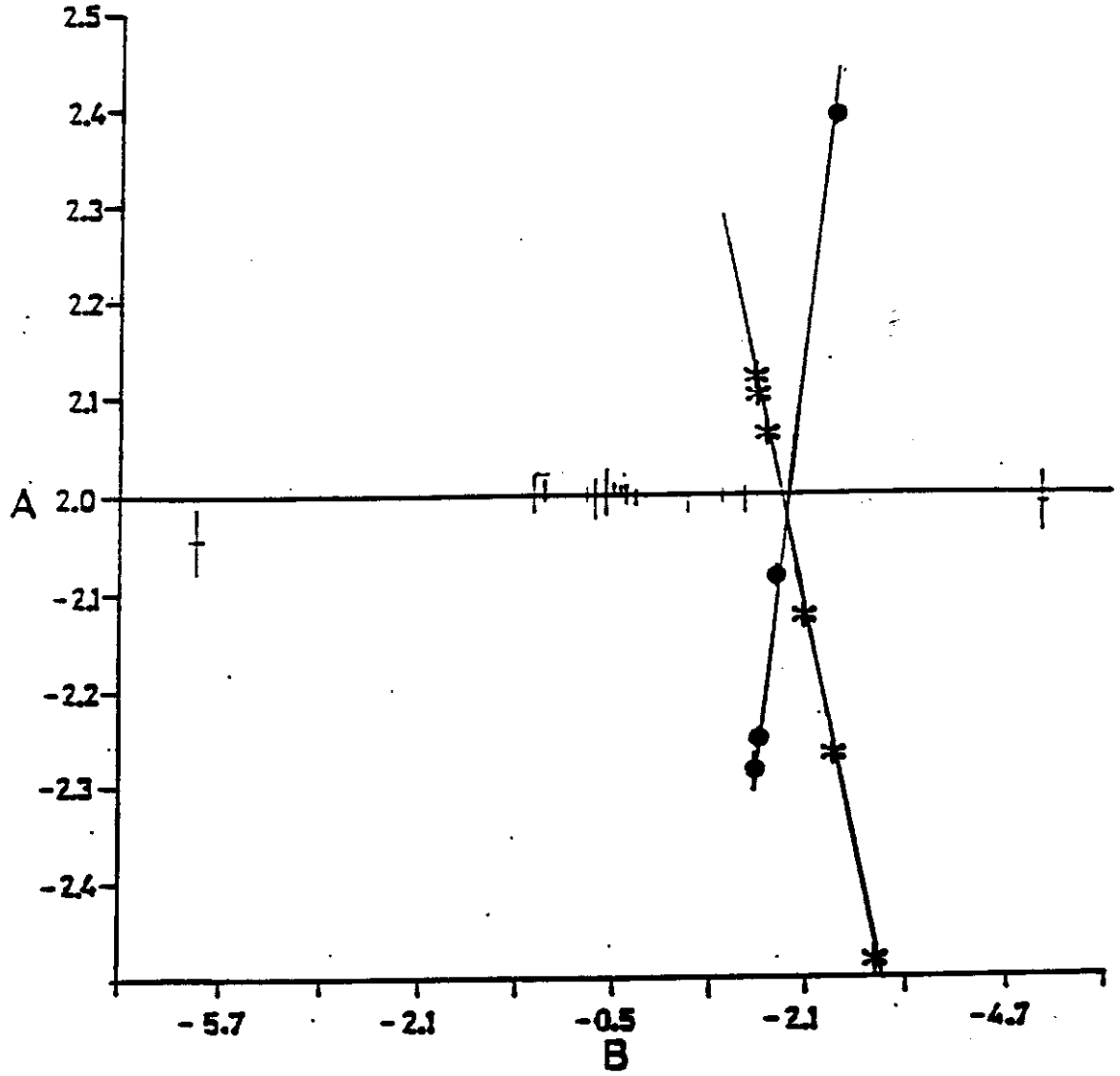

Figure 3.

The minimum signature of a secondary vertex is a track not coming from the main event vertex. In practice to localize a secondary vertex well we need at least three tracks. A convenient representation of the event is obtained by making use of the conjugate plane where each track in the real R, space is represented by a point . A straight line written in the form y=ax+b is represented in the conjugate plane by a point of coordinates (a,b). Tracks originating from the same vertex will be represented in the (a,b) plane by points lying on a straight line. Events with a single main vertex will generate a single straight line. If secondary vertices exist their tracks will be represented by points lying (in general) outside the main vertex line. These points can be associated into different straight lines. If these lines are found, the secondary vertices are found.

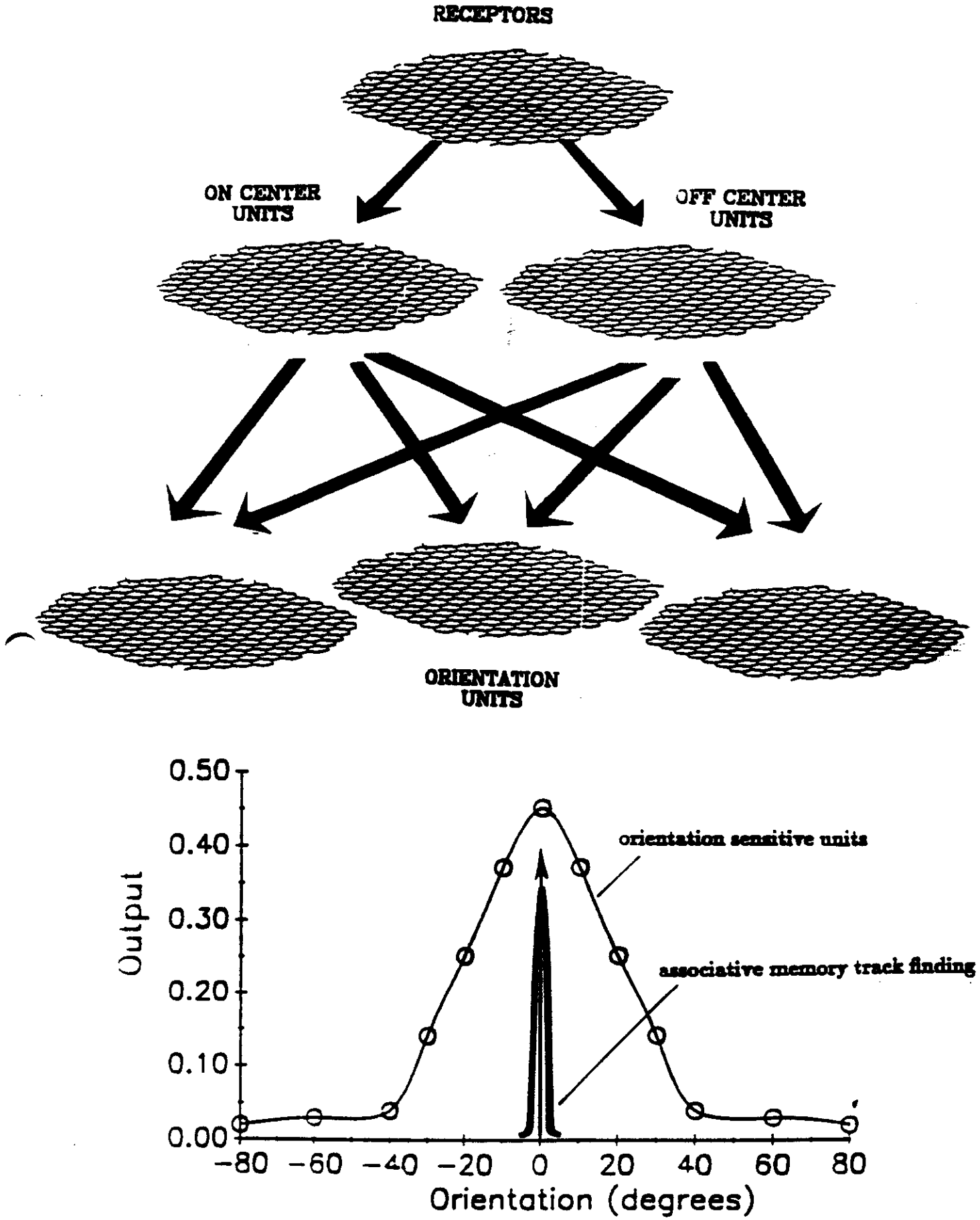

Figure 4. Constructing orientation selective cells from on-center cells, and comparison with associative memory track finding. From reference [17].